Journal of Materials Chemistry A

REVIEW

View Article Online
View Journal | View Issue

Cite this: J. Mater. Chem. A, 2019, 7, 23537

2D molecular crystal lattices: advances in their synthesis, characterization, and application

Marina A. Solomos,[a] F. James Claire[a] and Thomas J. Kempa *[ab]

Received 18th June 2019
Accepted 22nd August 2019

DOI: 10.1039/c9ta06534b

rsc.li/materials-a

This review identifies how recent advances in controlling the structure and properties of MOF and COF thin films can be used to establish 2D molecular crystals as a new material platform with key applications in catalysis, sensing, separations, and electronics. In addition to summarizing research efforts surrounding the synthesis, characterization and utilization of 2D and thin film MOFs and COFs, this review identifies exigent challenges in their development, and motivates the search for new synthetic methods, advanced analytical techniques, and creative applications. Ultimately, 2D molecular lattices, be they 2D MOFs or COFs, are a compelling platform through which to discover new and emergent properties and to expand the library of 2D materials.

1. Introduction

To appreciate the emerging opportunities in the study of two-dimensional (2D) molecular crystal lattices, one need only to look at the massive attention dedicated over the past 10 years to 2D atomic crystals. Graphene, graphene analogs of the group IV elements, and single-layer transition metal dichalcogenides are 2D atomic crystals that exhibit in-plane covalent bonding, out-of-plane van der Waals interactions with their surroundings, and electronic and optical properties that are distinct from those exhibited by their bulk counterparts.[1–7] These materials are frequently classified as van der Waals solids and can be combined with one another to yield so-called van der Waals heterostructures encompassing expanded or hybrid properties.[8]

In this vein, 2D metal organic frameworks (MOFs) and covalent organic frameworks (COFs) are a compelling platform on which to discover new emergent properties and expand the library of 2D materials (Table 1).[9–14] Two-dimensional molecular crystals can be synthetically designed and subsequently tuned to target a multitude of desirable material properties.[15–18] Porous by nature, 2D MOFs and COFs offer higher surface areas than conventional dense solids, heightened guest capture[19] and sensing[20] abilities, new charge transport modalities,[21] and improved catalytic performance.[22,23] Moreover, the extensive internal surfaces within MOFs and COFs can be post-synthetically modified to introduce additional tailorable functionalities.[15,24–27] Notably, the reduced dimensionality, the access to diverse bonding motifs, and the tunable symmetry and size of unit cells within 2D molecular lattices raises the

[a]Department of Chemistry, Johns Hopkins University, Baltimore, MD, USA. E-mail: tkempa@jhu.edu

[b]Department of Materials Science and Engineering, Johns Hopkins University, Baltimore, MD, USA

Marina Solomos earned her Ph.D. in 2018 from Georgetown University under the supervision of Prof. Jennifer A. Swift, where her research focused on controlling the crystallization behavior of polymorphic small molecules using functionalized templates and co-crystallization methods. In March 2018, she began her postdoctoral training at Johns Hopkins University with Prof. Thomas J. Kempa. Her current research explores vapor phase growth of coordination polymers for the development of responsive devices and sensors.

Jamie Claire received his B.S. in Chemistry from the College of Charleston in 2016. He is a Ph.D. candidate at Johns Hopkins University under the supervision of Prof. Thomas J. Kempa. His research focuses on the synthesis of responsive one- and two-dimensional metal–organic frameworks through solution and gas-phase methods and the investigation of their physical properties.

tantalizing prospect for design and discovery of new properties that could be leveraged to create a new generation of optoelectronic devices.[28–31]

The appeal of 2D MOFs and COFs, molecular nanosheets, and crystalline thin films is well established throughout the solid-state community, but significant challenges remain.[16,22,29,35–40] Past and current efforts consistently emphasize the need for improved thin film fabrication techniques. These methods must yield high-quality materials with minimal crystallographic defects and uniform surfaces, and must exert precise control over their dimensions.[41,42] Ideally, these methods should be scalable, facile, and cost-efficient to facilitate large-scale production of 2D molecular crystals. High-quality films of MOFs and COFs are defined as those having strong substrate interactions, uniform pore orientation, and well-defined layers.[43,44] In addition to these requirements, the preparation of singly- or highly-crystalline thin films over large areas is necessary for the integration of 2D molecular crystals into devices and other architectures.[43,45] New molecular systems and synthetic methods, or adaptations of existing synthetic methods, as well as new characterization techniques, are required to accomplish these goals.[23]

This review identifies how recent advances in controlling the structure and properties of MOF and COF thin films can be used to establish 2D molecular crystals as a new material platform with key applications in catalysis, sensing, separations, and electronics. Though many methods exist for the growth of polycrystalline, micrometer-thick MOF or COF films, to-date very few methods can grow high-quality crystalline thin films approaching the single-layer limit. Standard preparative routes target anisotropic crystal dimensions by inhibiting MOF or COF layer assembly (*e.g.* through interfacial synthesis and surfactant assisted growth), while substrate-directed growth methods rely on surface functionalization or patterning to template MOF and COF thin films as they grow layer-by-layer.[44,46,47] These "top-down" and "bottom-up" approaches have, in turn, led to a variety of promising techniques that improve thin film crystallinity and approach monolayer thicknesses by targeting the nucleation of molecular crystals. As the quality of 2D molecular crystals and thin films improves, their incorporation into multifunctional materials will be realized. The aim of this review is to summarize the state of research in 2D or near-2D MOFs and COFs, identify exigent challenges in their development, and motivate the search for new synthetic methods, characterization techniques, and creative applications.

Thomas (Tom) Kempa completed his Ph.D. studies in 2012 under the supervision of Prof. Charles M. Lieber at Harvard University. He then completed a post-doctoral fellowship with Prof. Daniel G. Nocera at MIT and Harvard. In July 2015, Tom joined the faculty of the Department of Chemistry at Johns Hopkins University as an Assistant Professor. Since 2017 he has held a joint appointment in the Department of Materials Science and Engineering. The Kempa group synthesizes and studies materials with novel structures, phases, and topologies and is currently focused on porous molecular solids, 2D materials, and multi-component nanostructures. These materials have unique properties rendering them useful for addressing outstanding challenges in fundamental science, energy sustainability, optoelectronics, and quantum information science. The Kempa group's expertise spans the areas of physical, inorganic, and materials chemistry. Tom has been the recipient of several grants and accolades including an NSF CAREER Award, a Toshiba Distinguished Young Investigator Award, and a Dreyfus Foundation Fellowship in Environmental Chemistry.

2. Synthetic advances

The fabrication of molecular nanosheets and thin films can be accomplished using either solution- or vapor-phase techniques. While preparative methods for nanosheets and thin films share some common features, it is important to understand the differences between the two material forms and how these differences influence their synthesis and utilization. Thin films range in thickness from several nanometers to micrometers and can be phase pure, layered, or mixed materials comprised of oriented or non-oriented crystalline grains. Preparing thin films of MOFs or COFs frequently involves interfacial reactions of separate monomer solutions or vacuum-assisted filtration of reacting components to assemble a compacted disk. In contrast, nanosheets are typically 2D monolayer or few-layer nanoscale lattices that can function as stand-alone materials or as components of a larger thin film or membrane.[22,48–50] The preparation of nanosheets may also be accomplished through interfacial, and other, reactions, but may also use techniques that limit the assembly of bulk MOF or COF crystals after nucleation. In this review, we include discussion of both nanosheet and thin film morphologies to emphasize the assorted applications of MOFs and COFs as they approach the scale of 2D materials.

When considering nanosheets and thin films of MOFs and COFs, optimized growth conditions specific to each unique framework are required. Though it is exceptionally challenging to prepare defect-free materials, the synthetic methods discussed herein offer diverse approaches for the formation of ordered MOFs and COFs as they approach the 2D scale and in many cases provide improved ordering compared to bulk growth methods. MOFs, assembled from metal nodes and organic linkers, can adopt 2D or 3D lattices and may require more carefully controlled coordination than COFs. As such, techniques that facilitate careful assembly of metals and linkers are better suited for MOF nanosheet and thin film growth, whereas the inherent 2D layering of COFs more easily allows for the manipulation of bulk phases towards 2D materials. MOF growth exploits slow diffusion of reactants, longer nucleation and growth times, higher boiling point solvents, and templating substrates.[51–53] COFs form 2D lattices from planar organic

Table 1 Summary of salient characteristics of 2D materials. Graphene scheme was adapted from ref. 32 and 2D transition metal dichalcogenide image is courtesy of Wang *et al.*, MIT.[33] 2D MOF scheme was adapted from ref. 34. COF image adapted with permission.[205] Copyright 2017 American Chemical Society

	Structural Features	Electronic Features	Applications
Graphene	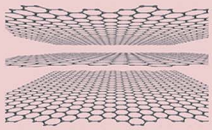 • One carbon atom thick layer (sp^2 hybridization) • Covalent bonds • Two atom unit cell • van der Waals interactions between layers	• Semimetal • Gate-tunable band structure • Topological properties	• Optoelectronics • Quantum phase transitions • Supercapacitors • Transparent conductive electrodes
2D TMD/oxides	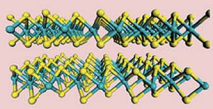 • Few atom thick layer • Covalent bonds • Small unit cells • van der Waals interactions between layers	• Mostly semiconductors • Layer tunable band-gap • Diverse exciton physics due to reduced dielectric screening and strong spin-orbit coupling	• Optoelectronics (*e.g.* FETs) • Quantum phase transitions • Photocatalysts • Valleytronics
2D MOFs	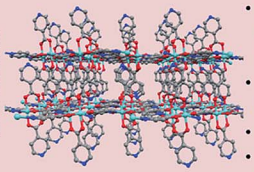 • Broad range of building unit motifs and lattice symmetries • Covalent and coordinate bonds • Large unit cells • van der Waals host-guest interactions	• Mostly insulators but with diverse range of electronic transitions (*e.g.* MLCT) • Through-framework conduction • Through-space conduction via mediators • Charge hopping	• Sensing • Gas and charge storage • Product separations • Catalysis • Protective coatings
2D COFs	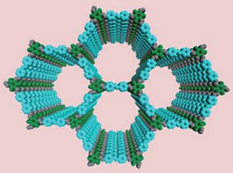 • Broad range of building unit motifs and lattice symmetries • Covalent bonds • Large unit cells • van der Waals host-guest interactions	• Tunable conductivity • Through-framework conduction • Through-space conduction via mediators	• Sensing • Gas and charge storage • Product separations • Catalysis • Protective coatings

linkers motivating the use of supramolecular design to introduce stronger layer interactions that lead to growth of high quality material.[54] COF growth can also be improved by simply altering modulator and reactant concentrations during assembly.[55]

2.1 Solution-phase methods

Solution-based synthetic methods for the preparation of crystalline thin films of molecular systems are well established. Bulk MOFs and COFs can be readily synthesized through straightforward mixing of monomer components in solution. MOF and COF crystal quality is closely dependent on the solvent used, the amount of heat introduced if using a solvothermal process, and the concentration of added monomers or modulators. Two-dimensional MOF or COF nanosheets are frequently synthesized from solution by adapting or expanding upon traditional solvothermal strategies employed for preparation of the corresponding bulk phases. As is the case during preparation of 2D atomic crystals, exfoliation of MOF or COF crystals is able to disrupt van der Waals contact forces and yield a layered lattice. However, gentler, solution-based exfoliation methods are often required to prevent substantial damage to the framework's crystalline structure. In many cases, the layered structure of MOFs lends itself well to simple sonication delamination.[56,57]

Banerjee *et al.*[36] synthesized two new bulk samples of imide-based COFs through standard solvothermal methods and subsequently sonicated these in isopropyl alcohol for 45–60 minutes. Centrifugation and drying of the collected material yielded covalent organic nanosheets with heights ranging between 1.5–5.1 nm, which corresponded to 5–15 COF layers. Initial wet ball-milling of bulk MOF crystals in methanol and propanol at slow speeds was shown by Yang *et al.*[23] to facilitate methanol penetration between constituent $Zn_2(bim)_4$ layers and to stabilize the resultant nanosheets prior to further exfoliation by sonication (Fig. 1a). The nanosheets have uniform thicknesses and are reported to be as thin as 1.12 nm, which is consistent with a monolayer. Sun and co-workers[58] recently reported a facile method for sonication exfoliation of a cobalt and pyrazine based MOF, $Co(CNS)_2(pyz)_2$, in ethanol for 30 minutes. The product was collected by rotary evaporation and was found to consist of monolayer nanosheets, which exhibited solvatochromic behavior and were subsequently implemented as solvent polarity sensors.

Chemical exfoliation methods have also been used to disrupt layered frameworks. PPF-1 MOF crystals, comprised of

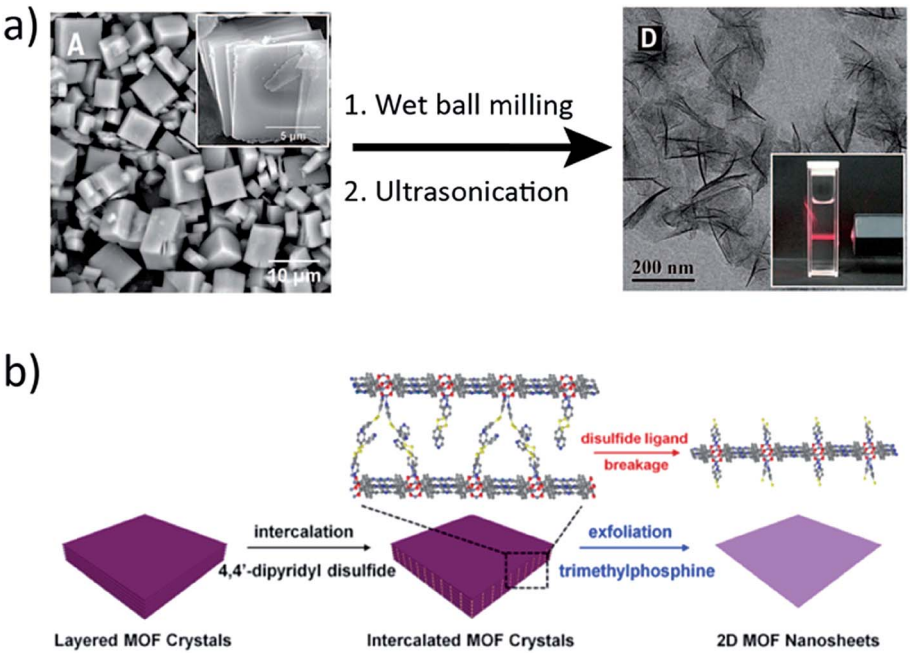

Fig. 1 (a) SEM image of as-synthesized $Zn_2(bim)_4$ crystals (left) which undergo wet ball-milling and ultrasonication to exfoliate single layers. TEM image of exfoliated nanosheets (right). The inset shows Tyndall scattering of the colloidal solution of nanosheets. (b) Schematic representation of the chemical exfoliation process using 4,4′-dipyridyl disulfide to produce single MOF nanosheets. Reprinted with permission from AAAS.[23] Adapted with permission.[59] Copyright 2017 American Chemical Society.

porphyrin sheets assembled from zinc paddlewheels, were exposed to 4,4′-dipyridyl disulfide to form a new, intercalated 3D MOF. Selective reduction of the disulfide bond by trimethylphosphine yielded ~1 nm thick MOF nanosheets. Zhou *et al.*[59] compared their method to surfactant-assisted exfoliation and found chemical exfoliation to be better suited for extracting single layer nanosheets (Fig. 1b). Similarly, Zhang *et al.*[60] designed a layered MOF incorporating 2,3-dihydroxy-1,4-benzenedicarboxylic acid as a redox-active pillar ligand. Selective oxidation of the pillar ligands realized conversion of the 3D MOF to ultrathin 2D nanosheets (~2 nm thick) in O_2 saturated electrolyte solutions. Delamination of $Cu_2(bdc)_2$ MOF crystals in oleylamine was demonstrated by Kaskel and coworkers[61] to yield ~70 nm thick sheets. The authors found that addition of polyvinylpyrrolidone, PVP, during crystallization of the parent $Cu_2(bdc)_2$ bulk phase yielded thinner (4–14 nm) 2D MOF sheets after exfoliation in oleylamine. Foster *et al.*[62] use a strategy of chemical design and ultrasonic exfoliation to prepare copper-based MOF nanosheets. They installed hydrophobic or hydrophilic pendant ligands in the parent bulk MOF phase and attempted exfoliation in solvents of ranging polarities. Sonication in acetonitrile for 12 hours yielded nanosheets as thin as 2–10 nm, and the authors found that nanosheet dimensions could be tuned through judicious choice of exfoliation solvent, sonication duration, and centrifugation time. COF nanosheets have also been produced by chemical exfoliation.[63–65] Banerjee and coworkers[66] combined post-synthetic modifications with a Diels Alder reaction to convert their anthracene-based COF to *N*-hexylmaleimide functionalized nanosheets, which were subsequently used to prepare thin films at an air–water interface.

Interfacial syntheses using solution phases of metal and/or linkers are another route towards the preparation of nanosheets and include strategies such as direct mixing, liquid–liquid layering, or three liquid layering processes. Inspiration for these strategies comes from success in preparing large area MOF and COF films of controlled thickness at vapor–liquid interfaces.[67,68] Tsapatsis *et al.*[69] showed that Cu(BDC) nanosheet formation is possible by mixing of copper(II) nitrate trihydrate in DMF and acetonitrile with a 1,4-benzenedicarboxylic acid solution. Either no mixing or gentle agitation formed ~25 nm thick Cu(BDC) nanosheets, which were readily collected by centrifugation. These nanosheets were then incorporated into mixed-matrix membranes, which exhibited an increased matrix selectivity for CO_2/CH_4. Thicker Cu(BHT) films were prepared by Zhu *et al.*[70] using a liquid–liquid interface reaction between aqueous copper(II) nitrate and benzenehexathiol in dichloromethane. The films, which can be clearly identified as forming at the interface, range in thickness from 20–140 nm, with thicker films exhibiting increased surface roughness. Films of 15–500 nm thickness were transferred to substrates and exhibited record conductivities ranging from 750–1580 S cm^{-1}. Comparable layering of monomer solutions was shown to prepare COF nanosheets as thin as 0.35 nm by Ma and coworkers.[71] Feng *et al.*[72] demonstrated the versatility of liquid–liquid interfacial synthesis by showing that the method could be used to prepare large-area thin films of a supramolecular organic framework prepared from truxene, 6-methoxynaphthalene, *N*-methyl-4,4′-bipyridin-1-ium, naphthalene diimide,

and cucurbit[8]uril. After a two hour assembly period in a custom-made glass trough, which facilitated layering of precursors, 1.8 nm thick monolayer sheets were isolated and transferred to Si/SiO_2 substrates. In recent work, interfacial synthesis has been used to prepare polyCOFs, covalent organic frameworks that incorporate linear polymers for heightened flexibility and lessened internal defects.[73] Zhang *et al.* prepared a water-soluble polymer that was mixed and layered with organic linkers and acetic acid catalyst, forming a free-standing membrane as thin as 4.5 nm.

Additional COF thin films were prepared by Dichtel *et al.*[74] through a process that involved first mixing all required monomers in a single organic phase and then layering with $Sc(OTf)_3$ catalyst in an aqueous phase. The resulting COF films covered a large area and had thickness ranging from 2.5 nm to 100 μm (Fig. 2). The authors found that film thickness could be controlled by changing monomer concentration, with low concentrations yielding thinner, less crystalline films. The COF films were used as the active layer in nanofiltration membranes, which were tested for their efficacy with micropollutant model compounds. Using a three-layer approach, Gascon *et al.*[75] demonstrated the formation of 5–25 nm thick Cu(BDC) nanosheets by separating layered solutions of the copper(II) nitrate and 1,4-benzenedicarboxylic acid precursors with an intermediate solvent layer. Slow diffusion of metal ions and BDC linker molecules forms MOF films within the intermediate layer. In yet another adaptation of liquid–liquid interfacial reactions, Su *et al.*[76] formed large area thin films of two new MOFs, Au_3BHT_2 and Ag_3BHT_2, by forming an organic solvent–water interface in a large dish with a SiO_2-coated silicon wafer resting at the bottom. Slow injection of a metal ion solution into the organic layer facilitated the formation of thin films of Ag_3BHT_2 and Au_3BHT_2 in 30 min and 6.5 hours, respectively. The MOF thin films were deposited onto the SiO_2 substrate through careful removal of the solvent. Though the films are several hundreds of nanometers thick and contain defects, the Ag-containing MOF exhibited a significant conductivity of 363 S cm^{-1}.

As seen in the examples above, interfacial synthesis is effective at limiting growth of molecular materials perpendicular to the interface and is therefore commonly used to prepare 2D MOF materials. The incorporation of a surfactant during nucleation and growth of MOFs has also been shown to be effective in encouraging the formation of nanosheets. Zhang *et al.*[77] developed a surfactant-assisted method for the formation of 2D Zn-TCPP MOF nanosheets. When introduced as a reagent during conventional MOF synthesis, polyvinylpyrrolidone (PVP) selectively attaches to zinc cations on the MOF surface and leads to anisotropic growth. Zn-TCPP nanosheets 7.6 ± 2.6 nm thick were achieved and correspond to 8 ± 3 layers of Zn-TCPP per nanosheet. Tsapatsis *et al.*[78] also demonstrated the utility of surfactant incorporation during MOF synthesis by mixing a metal precursor and ligand in a suspension of cetyltrimethylammonium bromide, CTAB, in heptane and hexanol. The selective binding of CTAB to the major crystal planes of Zn(Bim)OAc in conjunction with optimization of temperature conditions facilitates the formation of surfactant-free MOF nanosheets with 7 nm thicknesses (Fig. 3).

To enable their eventual incorporation into more functional materials and devices, MOF nanosheets must be either transferred to or selectively grown on substrates. Adapting the layer-

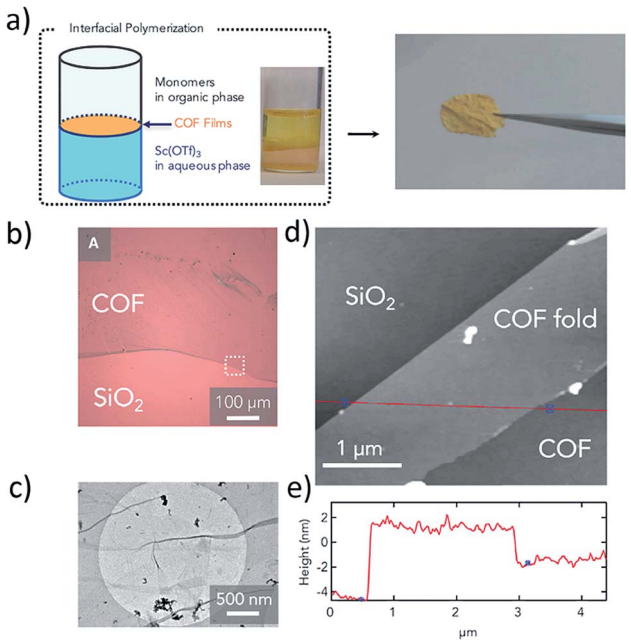

Fig. 2 (a) Schematic and photograph of liquid–liquid interfacial synthesis process (left) used to prepare TAPB-PDA COF and the resulting free-standing film (right). (b) Optical and (c) TEM micrographs of TAPB-PDA COF transferred onto Si/SiO_2 substrate and TEM carbon grids, respectively. (d) AFM image (white box from (b)) of isolated monolayer sheets and (e) height profile along the red line in (d). Adapted with permission from Elsevier.[74]

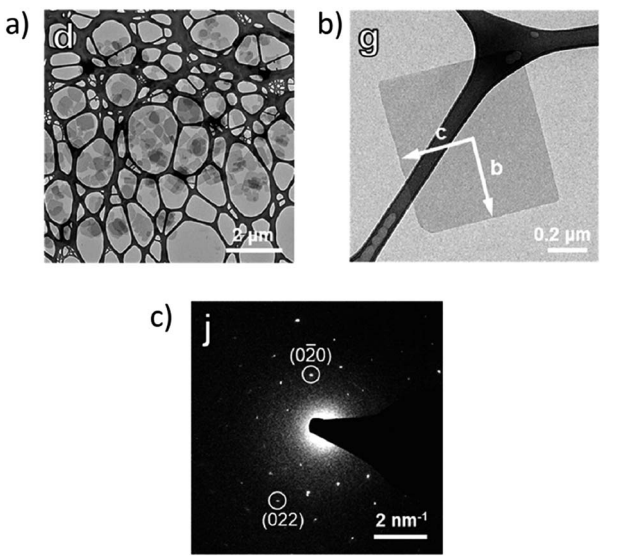

Fig. 3 TEM images of (a) several nanocrystals and (b) a single nanocrystal of Zn(Bim)OAc synthesized in a suspension of CTAB in heptane and hexanol at 25 °C. (c) Corresponding electron diffraction pattern of a single nanocrystal. Adapted with permission.[78] Copyright 2018 American Chemical Society.

by-layer process (LbL), Kitagawa *et al.*[79] utilized standard solvothermal techniques to prepare nanoflakes of a range of MOFs. In one example, the authors prepared Cu-TCPP nanoflakes, approximately 15 nm or 33 porphyrin layers in thickness, suspended them in ethanol, and then added them dropwise to the surface of water, thereby assembling a thin film which could be transferred to assorted substrates through a simple stamping process. Characterization of the thin film revealed that it has a crystallinity and orientation similar to that of the SURMOF bulk phase. Coronado *et al.*[80] prepared MOF thin films as thin as 10 nm by dipping functionalized substrates (silicon, gold, and permalloy) into a CoTCPP-pyridine solution, which had been dispersed over a copper(II) nitrate solution. The functionalized substrates successfully directed the transfer of MOF nanosheets onto suitable interfaces for device integration, whereas bare substrates exhibited poor or failed transfer.

As an alternative to the transfer of MOF films onto substrates, MOF or COF thin films can be directly grown on selected regions of a substrate if the desired areas are pre-functionalized with self-assembled monolayers (SAMs).[81,82] Wöll *et al.* demonstrated the utility of functionalized substrates for the bottom-up assembly of MOF thin films.[44,83–85] Gold surfaces functionalized with 11-mercapto-1-undecanol were subjected to sequential, layer-by-layer (LbL) depositions of metal and ligand solutions (liquid phase epitaxy), with growth cycles monitored by a quartz crystal microbalance (QCM). Resultant MOF films were 64–80 nm thick and were intentionally loaded with assorted metal ions. Further work on carboxylate-functionalized Au surfaces showed that MOF thin films with similar thicknesses can be prepared by spray coating metal and ligand solutions sequentially. Performing LbL growth on QCMs, Allendorf *et al.* have shown that both functionalized semiconductor surfaces[86,87] and patterned substrates[88] are able to facilitate growth of two or three unit cell thick, stacked crystalline MOF sheets of HKUST-1. While monitoring the MOF assembly process with QCMs, Fischer and coworkers[89] alternately deposited $Zn_4O(OAc)_6$ solution and various 3,5-dialkyl-4-carboxypyrazolate linkers onto functionalized gold sensors to form crystalline thin films of $[Zn_4O]^{6+}$ MOFs. The influence of acetic acid modulators, which are added to either the metal or ligand solutions prior to LbL assembly, on the crystallinity of the thin films was assessed. Marks, Stoddart, and colleagues[90] prepared gamma-cyclodextrin (CD) self-assembled monolayers to facilitate the epitaxial growth of CD-MOF polycrystalline thin films on glass substrates. The large-area surface coverage and oriented growth (2 μm) of these films allowed for their direct incorporation into a functional device with enhanced proton conductance and CO_2 sensing abilities. Hupp[91] also prepared surface-supported, patterned films of ZIF-8 for the formation of hybrid materials with vapor sensing capabilities.

Unfunctionalized substrates can still aid in the formation of well-adhered MOF thin films by acting as metal ion sources in the presence of organic linkers and oxidizing or deprotonating agents. Jeong *et al.*[92] showed that copper and zinc substrates are able to seed the growth of HKUST-1 and ZIF-8, respectively. The HKUST-1 film thus prepared exhibited an increased conductance in the presence of I_2 suggesting its utility as a sensor. Interestingly, graphene oxide has been shown as a viable template for MOF growth, binding HKUST-1 and facilitating continuous thin film growth *via* a rod-like intermediate.[93] Kunitake and coworkers[94] showed that graphite substrates facilitated the formation of large nanosheets of Cu-H_2TCPP with sub-1 nm thicknesses in the presence of acetic acid vapor.

A number of strategies have been explored to streamline and industrialize MOF growth processes using automated deposition methods such as spray coating or spin coating. Behrens and co-workers[95] demonstrated the use of ammonia modulation to prepare nanoflakes of Cu_3HTTP_2 that were subsequently deposited manually/automatically onto substrates by spray-coating to create homogenous oriented films, which could serve as protective coatings. Eddaoudi *et al.*[96] developed a spin coating method for the preparation of thin films of assorted MOFs by multilayer deposition. Their apparatus consisted of four micro-syringes capable of depositing metal ion and linker solutions onto rotating substrates to produce uniform thin films ranging in thickness from several nm to μm (Fig. 4). Farha and Hupp[97] precisely controlled the thickness of their MOF

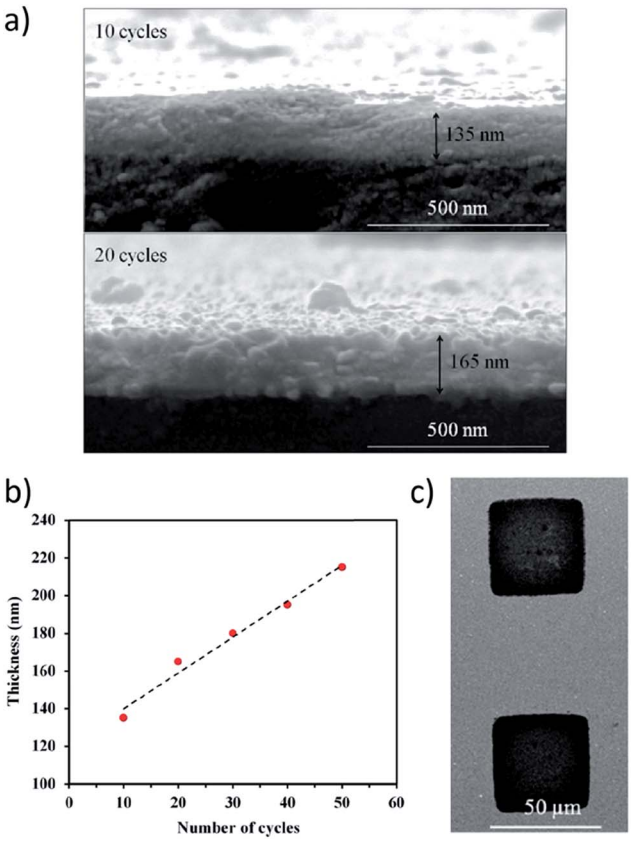

Fig. 4 (a) SEM images of the cross-section of $Cu_2(bdc)_2 \cdot xH_2O$ MOF thin films deposited using the four micro-syringe spin-coating method after 10 (top) and 20 (bottom) cycles. (b) Height profiles of thin films produced after 10 to 50 cycles. (c) Substrate-selective growth of MOF on patterned substrates during the spin-coating process. MOF thin films only form within the square patterned regions having COOH-terminated surfaces. Deposition on CH_3-terminated areas of the substrate is negligible. Adapted with permission.[96] Copyright 2016 American Chemical Society.

films by alternately soaking amino-functionalized silicon substrates in separate solutions containing Zn^{2+} ions and different ligands. The process was automated to enable precise control over the number of cycles and likewise the film thickness. Thomas *et al.*[98] developed a flow synthesis method that confines the reaction of MOF precursor solutions within droplets, which form upon injecting the solutions into an oil phase. The droplets flow through a heated microchannel, which also prevents layered growth of the MOF crystals, at the end of which ultrathin 2D nanosheets of ZrBTB MOFs are collected. Height profiles reveal the sheets to be as thin as 3–4 nm, corresponding to 3–4 crystallographic layers.

Substrate-mediated techniques have demonstrated their efficacy for high quality growth of molecular thin films, but more recent solution-based methods focus on adjusting the nucleation kinetics of MOFs and COFs in an effort to control crystal growth. Dichtel and colleagues have recently shown that colloidal suspensions of COF-5 seed crystals can grow larger, high quality single crystals when monomer addition takes place slowly.[99] In related work, Dichtel *et al.* also showed that COF-5 thin films could be controllably prepared in a flow cell.[100] Monomers added to a small volume of methanol within their flow cell apparatus formed COF-5 thin films within minutes. The films exhibit minimal contamination with bulk aggregates and their thickness and crystallinity can be controlled by the residence time of the monomer within the apparatus, the monomer concentration, and the reaction temperature. Yaghi *et al.*[101] employed an *in situ* deprotection step to better control the nucleation stage of imine-based COFs, such as LZU-1. This process favored the nucleation of oriented nanocrystals on silicon substrates and formed thin films, which were approximately 190 nm thick (Fig. 5).

2.2 Vapor-phase methods

Though preferred by most researchers, solution-based growth struggles to afford a high degree of control over thin film quality just as solvent-based bulk recrystallization of MOFs and COFs remains a perennial challenge. Numerous problems conspire against the formation of consistently high-quality MOF and COF thin films, including the formation of defects, polycrystalline domains, metastable phases, and macroscale cracks. To address many of these concerns, as well as eliminate unwanted solvent effects, the preparation of thin film molecular crystals *via* gas phase methods has recently gained attention as a promising approach to the deposition of uniform layers of molecular materials with control of thickness. In combination with patterned templates or functionalized substrates, the discovery of molecular framework systems capable of forming ordered crystalline thin films from the gas-phase has the potential to transform 2D molecular crystal studies.

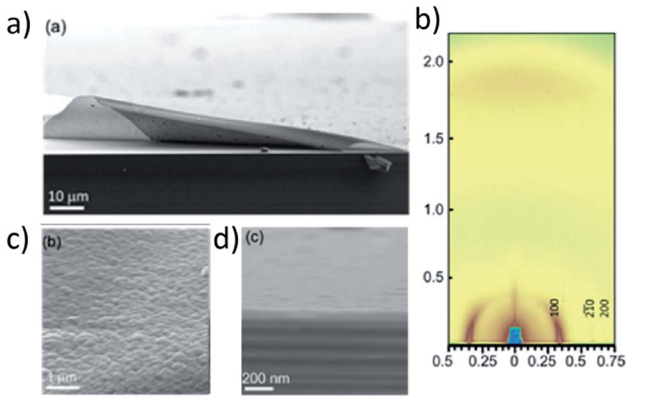

Fig. 5 (a) Highly uniform thin film of LZU-1 synthesized with *in situ* deprotection. (b) The crystallinity and orientation are confirmed by GIWAXS. (c) The thin film is composed of small crystallites with similar orientation and is 190 nm thick as measured by (d) cross-sectional SEM. Adapted with permission.[101] Copyright 2017 American Chemical Society.

Just as atomic layer deposition (ALD) and chemical vapor deposition (CVD) are commonly used for the synthesis of 2D materials,[102,103] molecular layer deposition (MLD) and CVD are now becoming attractive candidates for the preparation of high-quality crystalline MOF and COF thin films.[104–107] Ritala *et al.* prepared MOF-5 thin films by ALD[108] through iterative application of zinc acetate and 1,4-benzenedicarboxylic acid precursor pulses within a hot wall reactor. The initially deposited amorphous material was transformed into MOF-5 upon water vapor exposure. Ameloot and coworkers have further demonstrated the promise of solvent-free preparative routes. They showed that heating a zinc oxide film covered with a thin layer of 2-methylimidzaole to 433 K produces ZIF-8 within one minute.[109] More recently, Ameloot *et al.* used CVD[110] to deposit zinc oxide on a range of flat and textured substrates, and then treated these substrates with 2-methylimidazole vapor under ALD conditions (Fig. 6a and b). This two-step process yielded continuous 52–104 nm thick ZIF-8 polycrystalline films (Fig. 6c). Boroxine COF monolayers were prepared by Lackinger *et al.* through sublimation under ultra-high vacuum conditions.[111] Characterization with STM revealed hexagonal networks and lattice parameters in good agreement with COF monolayers. The modification of larger precursors was occasionally required to facilitate sublimation and, in some instances, exposure to water vapor was needed to induce COF formation.

In our own work, we have utilized a single-step CVD reaction to grow ultra-thin single crystals of a MOF comprised of dimolybdenum paddlewheel clusters.[34,112,113] These high quality and phase pure single crystals have exceptionally uniform surfaces, are highly oriented, and can be mechanically exfoliated to yield thin films with thicknesses approaching several nanometers (Fig. 6d). Our work represents the first effort to prepare singly crystalline MOF thin films directly (*i.e.* not requiring subsequent conversion) from the gas phase. Notably, we discovered unique phase and electronic switching properties in our MOF by monitoring *in situ* the response of devices we fabricated from single crystals of this MOF.

Challenges remain with regards to the widespread use of vapor phase growth methods for framework materials. Sublimation temperatures of monomers or precursors may be difficult to determine if complete or partial decomposition occurs, and widely different sublimation temperatures of individual components may necessitate multi-step growth processes.

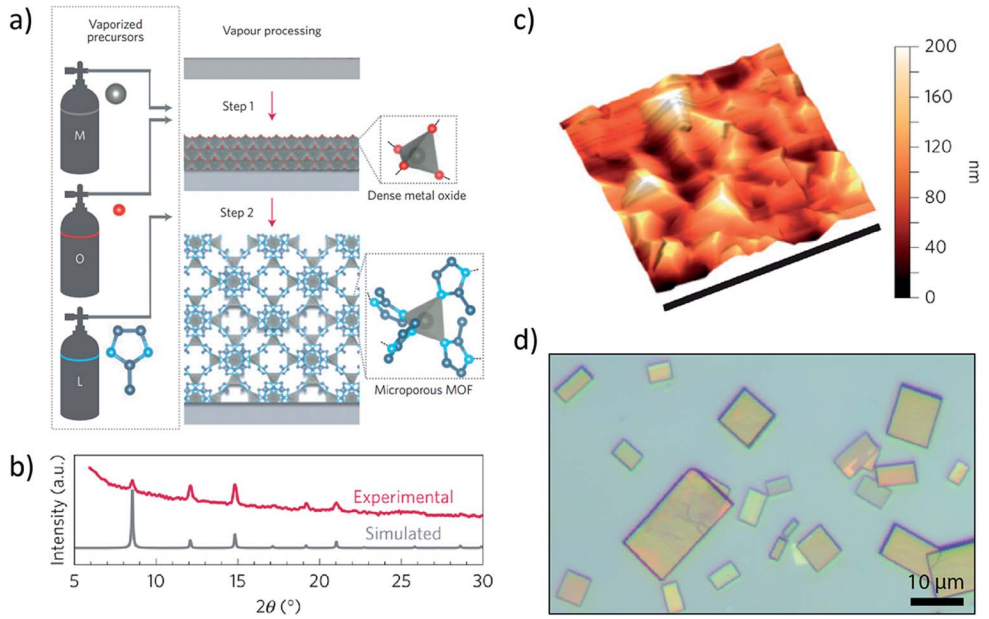

Fig. 6 (a) Schematic representation of CVD synthesis of ZIF-8 through a two-step process involving deposition of a dense metal oxide followed by introduction of organic ligand. (b) Conversion of ZnO to ZIF-8 confirmed *via* comparison of measured and simulated pXRD patterns. (c) 3D rendered AFM topograph of a polycrystalline film of ZIF-8. (d) Optical images of single crystals of our $Mo_2(INA)_4$ MOF synthesized directly through a one-step CVD reaction.[112] Adapted by permission from Springer Nature[110] Copyright 2016.

Moreover, the initially deposited material may be amorphous and difficult to subsequently crystallize. Finally, coordination of precursors in the gas phase or following their adsorption onto substrates may be difficult in the absence of catalysts. However, we foresee expanded use of gas-phase methods, including CVD, for the preparation and fundamental investigation of high-quality MOF and COF thin films, particularly if novel precursors or frameworks suitable for gas phase growth are developed. We also see an exciting opportunity for facile integration of these diverse materials into devices, including sensors, actuators, and detectors.

3. Characterization

Thorough characterization of 2D or nearly-2D molecular materials is of paramount importance in the quest to discover promising properties that may manifest within these materials, and in the ongoing effort to develop new synthetic strategies to address the exigent challenges discussed above. Several features of a MOF/COF thin film or few-layer nanosheet must be determined in order to inform its subsequent application: (1) film quality, (2) material phase, (3) nanosheet dispersion, (4) stability, and (5) pore size. Most bulk MOF and COF characterization techniques can be translated to the analysis of dimensionally restricted materials without requiring major modification. However, careful attention must be paid to data quality and interpretation of results, because sample variability can introduce systematic errors and because properties measured on bulk materials may be significantly altered when the same material takes on a nanoscale dimension. Though tedious, multiple nanosheets or thin films should be individually characterized to build a robust, statistically-significant dataset. Furthermore, powerful *in situ* techniques—which may need to be modified or developed specifically for 2D molecular materials studies—will aid in assessing the aforementioned features during synthesis and device fabrication.

Solution-phase characterization is often used for facile and initial assessment of nanoscale materials. Most analyses can be accomplished immediately after synthesis in the reaction vessel or following sample re-suspension in a nonreactive solvent. Tyndall scattering, UV-visible absorbance spectroscopy, and dynamic light scattering (DLS) are bulk techniques used to assess the dispersity of exfoliated MOF and COF samples. Tyndall effect scattering upon laser irradiation of a material dispersion can be readily quantified and, unsurprisingly, has featured prominently in the analysis of many nanosheet and thin film samples (Fig. 7a).[23,114,115] Though this technique confirms a suspension of nanoscale particles, the contribution of particle sub-populations cannot easily be discerned. For size distribution analysis, DLS can be used to obtain the average diameters of MOF and COF nanosheet dispersions.[116] UV-visible absorbance (UV-Vis) spectra—solution based or solid-state—may be employed to confirm formation of a MOF or COF thin film.[72] Liu *et al.*[117] used UV-vis absorbance to monitor the complexation of zinc ions and TCPP by observing a red shift in the ligand's Soret band. A distinct shoulder on the Soret band developed as Zn-TCPP MOF nanodisks formed, with absorption intensity correlating to particle size as a function of modulator inclusion during the crystallization process. Indicating the prevalence of these techniques, Foster *et al.* recently used all three techniques—Tyndall scattering, DLS, and UV-vis spectral

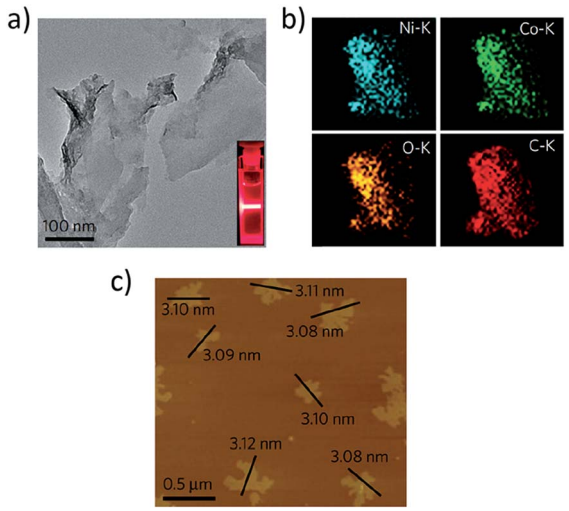

Fig. 7 (a) TEM image of NiCo-UMOFNs with optical image of Tyndall light scattering (inset) upon laser irradiation. (b) EDS elemental mapping of NiCo-UMOFNs obtained within a TEM. (c) AFM map of individual NiCo-UMOFN flakes. Adapted by permission from Springer Nature.[115] Copyright 2016.

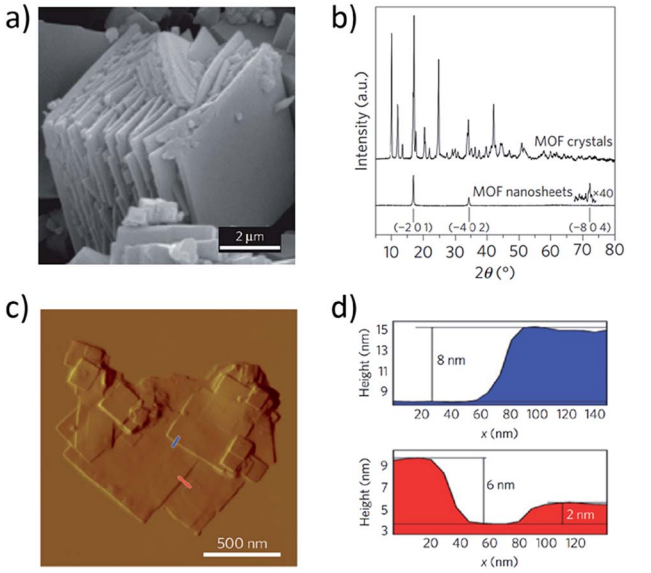

Fig. 8 (a) SEM image of bulk CuBDC MOF crystals comprised of layered nanosheets. (b) pXRD scans of bulk CuBDC MOF crystals and corresponding nanosheets. (c) AFM map of MOF nanosheets. (d) Height profiles taken along the paths indicated in (c). Adapted by permission from Springer Nature.[75] Copyright 2015.

intensity—to assess their post-synthetic exfoliation method for the preparation of ultrathin, catalytic nanosheets.[118]

Since single crystal X-ray diffraction is usually impossible due to the inherently restricted dimensionality of nearly-2D molecular films, these materials are frequently characterized with powder X-ray diffraction (pXRD). pXRD allows for relatively straightforward assessment of sample crystallinity, phase, and layering/lattice spacing, but often requires bulk samples, which may not be representative of the individual films, and a known crystal structure to serve as a reference (Fig. 8a and b).[75] Though Aida *et al.*[119] were successful in obtaining single crystal structures of their self-exfoliating Cu(II) MOF, pXRD proved useful in studying the accordion-like expansion process their MOF was able to undergo. Upon exposing their MOF to THF vapor, the authors observed an interlayer expansion that was represented by large shifts of the (001) peak in 2θ. This result corroborated previously observed large increases in the interlayer d-spacing from 6.8 Å to 17.0 Å prior to self-exfoliation. Wöll *et al.*[120] employed out-of-plane pXRD to assess the lattice-constants of their liquid-phase epitaxially-grown, heterostructured SURMOFs and to confirm the orientation of their thin film. pXRD can also be used to monitor growth processes and the effects of modulators on film phase, as Ameloot *et al.* did in monitoring acetic acid vapor modulation on UiO-66 films.[121] Synchrotron X-ray diffraction and grazing incidence X-ray diffraction (GIXD) can provide additional information regarding the surface crystallinity and multi-layer composition of a thin film.[122,123]

Though useful, diffraction techniques are not always well suited to provide information regarding film composition. Given its inherent surface sensitivity, X-ray photoelectron spectroscopy (XPS) is often used to identify both the elemental composition and the metal-linker coordination on the surface of molecular nanosheets.[39,124,125] Other characterization methods that provide chemical information include Fourier-transform infrared (FT-IR), Raman,[72,117,126] and solid state nuclear magnetic resonance (NMR) spectroscopies.[127,128] Also commonly used in the MOF and COF community, Brunauer–Emmett–Teller (BET) analysis probes the pore structure of thin films and nanosheets by fitting their gas adsorption–desorption[95,104,129,130] isotherms. Calculated surface areas from BET analysis indicate the accessible pore volume of MOF and COF materials and are used to compare these materials on the basis of their gas storage potential or permeability.

In contrast to these aforementioned techniques, which are most often performed on bulk quantities of sample, optical microscopy and atomic force microscopy (AFM) are most informative when deployed on individual specimens or distinct and smaller regions of a sample. Optical microscopies, especially those encompassing dark-field and phase-contrast imaging, are useful for visualizing film quality and surface defects in larger crystals or large-area thin films, though probe depth and resolution are defined by the energy and intensity of the optical beam, parameters of the microscope optics, and the Abbe diffraction limit. Zhao *et al.* could clearly observe the surface roughness of their millimeter-wide Cu-TCPP thin films by visualizing regions having different textures and color saturations.[131] Atomic force microscopy (AFM) is considerably more useful for analyzing the surface roughness and thickness of nanoscale thin films. Most analyses of exfoliated thin film MOFs and COFs utilize AFM to measure the step-heights of individual layers within a multi-layer film (Fig. 7c, 8c and d).[57,75,115,132,133] The angstrom-level z (height) resolution of AFM facilitates comparison of AFM acquired step-heights to known crystal lattice spacings, provided that the 2D layers are properly oriented.

Electron microscopy, which encompasses a range of advanced techniques including scanning electron microscopy

(SEM), transmission electron microscopy (TEM), scanning transmission electron microscopy (STEM), and, most recently, *in situ* and aberration-corrected TEM/STEM, is used to obtain high-resolution to atomic-resolution data of ultrathin molecular materials. The insulating nature of many MOFs and COFs presents imaging challenges, though many of these can be overcome through the use of conductive support films and coatings, which provide effective charge dissipation. The complementary resolution levels of SEM and TEM images provide excellent structural insight across multiple length-scales. SEM often lends morphological insight regarding the likelihood that a sample can be readily exfoliated[114] and TEM provides an assessment of the crystallinity and inter-layer alignment within multi-layer films.[128] When combined with energy-dispersive X-ray spectroscopy (EDS), SEM or TEM can also provide elemental mapping of the sample's surface (Fig. 7b).[39,115,134,135] Yang *et al.*[23] clearly show the flake-like, layered morphology of their bulk $Zn_2(bim)_4$ single crystals and provide TEM images of the impressively thin nanosheets obtained after wet-ball milling and ultrasonication (Fig. 1a). Thomas *et al.*[98] similarly show SEM and TEM images of their MOF nanosheets prepared through microdroplet flow reaction. High resolution TEM (HR-TEM) images of their MF-ZrBTB nanosheets show clear lattice fringes with Zr_6 clusters consistently spaced apart by the expected lattice distances, thereby suggesting good crystallinity of their nanosheets. Selected-area electron diffraction (SAED) can be performed during TEM data collection to assess the local crystallinity of sufficiently thin samples. Diffractograms obtained through SAED can be compared to known crystal structures in order to index crystalline grains or local phases in MOF or COF samples.[116] Advanced dark-field imaging techniques, notably high-angle annular dark-field and precession diffraction-based imaging, can provide exceptionally detailed information as to how the phase, orientation, and defect density vary across a thin sample. Care must be taken to employ imaging conditions (*e.g.* acceleration voltages and beam currents) that do not degrade the MOF or COF samples, with low-kV imaging being of particular utility in this regard. Though less frequently used, scanning tunneling microscopy (STM) is a powerful technique that allows for the imaging of single MOF or COF layers on metal substrates and provides atom-level resolution and electronic structure information at the monolayer level.[136–139]

The choice of characterization technique can also be guided by the intended application of the 2D nanosheet. For some systems, magnetic susceptibility measurements are useful for investigating electronic structure and bonding. Gómez-García and coworkers identified ferromagnetic Fe–Fe interactions in their MOF systems likely arising from mixed-valency of the Fe(II)/Fe(III) lattice.[56] For these and other functional MOF and COF systems, authors are increasingly providing charge transport measurements.[95,140–142] We recently assessed the conductivity of our dimolybdenum isonicotinate crystalline thin film devices. Current–voltage characteristics obtained from these devices identify a conductivity of 2.25×10^{-8} S cm^{-1}, which increases by 8-fold under laser illumination. Notably, we observe a large increase in conductivity to 6.22×10^{-7} S cm^{-1} while monitoring conversion of the crystal *in situ*.[112]

Indeed, the fact that crystalline thin films and nanosheets can change their phases and associated properties mandates the development and use of *in situ* characterization methods to monitor and potentially control solid-state transitions.[143] More importantly, *in situ* analysis of MOF and COF thin film growth would provide valuable insights regarding plausible mechanisms for formation of these coordinated frameworks. In turn, such studies could inform design and optimization of reactions to achieve higher quality 2D molecular materials. An assortment of *in situ* X-ray diffraction techniques is currently available but their widespread use is limited.[144] For example, *in situ* high energy, X-ray atomic pair distribution function analysis can monitor nucleation by providing structural information as precursors mix but requires a synchrotron source.[145] When paired with *in situ* TOF-SIMS spectroscopy, however, the assembly and modification of molecular species in solution can be monitored.[145] Methods to monitor morphology and crystallinity, such as *in situ* SEM[146] and TEM,[147] exist and are employed for 2D atomic materials but have not been readily used for analysis of molecular systems. Weckhuysen *et al.* developed an *in situ* AFM method and used it to monitor HKUST-1 thin film growth by observing a 10×10 μm section of Cu-BTC solution deposited on a functionalized Au substrate.[148] Nucleation of copper and BTC linker was observed and HKUST-1 grain formation could be monitored at several temperatures. In an effort to provide chemical information, Parsons *et al.* developed an *in situ* technique for attenuated total reflectance infrared spectroscopy.[149] The formation of HKUST-1 was monitored by examining the conversion of ZnO and $Cu(NO_3)_2$ to the MOF upon addition of H_3BTC. The symmetric and asymmetric stretching modes of the HKUST-1 carboxylate groups were monitored every 0.49 seconds. Continued development of *in situ* characterization techniques for 2D molecular materials will undoubtedly advance further investigation of these systems.

4. Applications

While researchers continue to explore the potential of true 2D MOFs and COFs, these materials have demonstrated impact in a number of electronics, energy storage, catalysis, and biomedicine applications. The plethora of fundamental studies and applications enabled by 2D atomic crystals bodes well for the potential impact of 2D molecular frameworks, which allow for an exceptional degree of freedom in chemical design. We anticipate that collaboration between the solid-state, inorganic, and condensed matter communities will spawn new research areas with extraordinary potential. Here, we highlight some of the current, innovative applications using 2D or nearly-2D molecular materials, as well as some hybrid materials. Notably, not all cited work focuses exclusively on nanoscale or monolayer molecular materials. Research focused on thicker, microscale thin films is valuable and welcome as findings from these systems provide important insights towards the development and scale-up of more dimensionally restricted molecular materials.

4.1 Catalysis

2D MOF and COF materials are candidate heterogenous catalysts for the hydrogen and oxygen evolution reactions (HER and OER) and for small molecule activation. Marinescu *et al.*[150] deposited thin films of their cobalt dithiolene catalysts onto assorted substrates and reported an overpotential of 530 mV at 10 mA cm^{-2} for this thin film catalyst that is lower than that for the bulk molecular material. In related work, Feng and coworkers[151] prepared a single-layer sheet of their nickel bis(dithiolene) complex and measured an overpotential of 333 mV at 10 mA cm^{-2}. More recently, Marinescu *et al.*[152] reported a record hydrogen evolution activity from one of a series of benzenehexathiolate (BHT) coordination framework films. Compared against NiBHT and FeBHT, CoBHT films generally produced the lowest overpotential of 185 mV with film thicknesses of ~244 nm. Stacked sheets of CoBHT were observed at thicknesses as low as 20 nm and as high as nearly 1 μm, but these thicknesses were found to produce larger overpotentials.

As part of a further development of electrocatalysts to mediate HER, Nishihara *et al.*[153] prepared bis(iminothiolato)nickel (NiIT) nanosheets, where an increase in conductivity from 3×10^{-6} to 1×10^{-3} S cm^{-1} was ascribed to preparation of the authors' NiIT material as a nanosheet. The NiIT nanosheets were then employed as HER electrocatalysts and reported to have an onset overpotential of −0.15 V *vs.* RHE and an operating overpotential of −0.37 V at 10 mA cm^{-2}. Qiao and coworkers[154] prepared a catalytically-active hybrid Co-BDC/MoS_2 material by exposing exfoliated MoS_2 nanosheets to $CoCl_2 \cdot 6H_2O$ and BDC solutions. These hybrid nanosheets demonstrate heightened HER activity in alkaline electrolytes with an onset overpotential of 155 mV. This overpotential is lower than would be the case with either component in isolation. To achieve current densities of 10 mA cm^{-2}, the Co-BDC/MoS_2 nanosheets required only 248 mV of overpotential. Moreover, even after the acquisition of 2000 cyclic voltammograms, the nanosheets exhibited good stability.

Tang *et al.*[115] prepared ultrathin mixed-metal NiCo MOF nanosheets (approximately three structural layers) and tested their efficacy as catalysts for OER. When the NiCo nanosheets were deposited on glassy-carbon and on copper foam, the overpotentials required to achieve a 10 mA cm^{-2} current density were measured at 250 mV and 189 mV, respectively. The NiCo MOF nanosheets also exhibit a significantly higher turnover frequency compared to either monometallic (Ni or Co containing) nanosheets or the bulk mixed-metal phase. Zhang *et al.* produced 2 nm thick nanosheets of their pillared cobalt framework, as previously described,[60] and reported low overpotentials (211 mV at 10 mA cm^{-2}) and high turnover frequencies. Similarly, Zhao *et al.*[155] measured a 240 mV overpotential at 10 mA cm^{-2} for OER with their NiFe MOF nanosheets. When assessing the activity of this material for HER, they observed a 134 mV overpotential. The NiFe-MOF nanosheet was then used as both the anode and the cathode in experiments assessing its efficacy in electrocatalytic water splitting. At an operating voltage of 1.60 V, H_2 and O_2 bubbles could be seen at the cathode and anode, respectively. Recently, Lang *et al.*[156] also produced nanosheets of mixed metal MOFs for OER. NiFe MOF nanosheets, solvothermally synthesized from $Ni(OAc)_2 \cdot 4H_2O$, $Fe_3SO_4 \cdot 7H_2O$, and 1,4-H_2BDC, were measured to be 1.67 nm to 2.58 nm thick. The nanosheets produced an overpotential of 221 mV at a current density of 10 mA cm^{-2}, and were judged to perform better than monometallic MOF and commercial Ir/C. While other mixed metal nanosheets were prepared (*e.g.* comprising Al, Co, Mn, Zn, and Cd), the Fe-containing MOF exhibited the most impressive OER activity and stability, with only minimal changes in activity over 1000 CV cycles.

Dincă *et al.*[157] prepared conductive thin films of $Ni_3(HITP)_2$ on electrode surfaces and assessed their efficacy as catalysts for the OER. Films ranging from 120 nm to 300 nm thick, supported on either glassy carbon electrodes or indium tin oxide, produced an overpotential of 0.18 V (relative to Pt) and reduced oxygen with an onset potential of 0.82 V in 0.1 M KOH. Analysis of the thin films before and after reaction revealed marked stability of the catalyst. Yang, Yaghi, and coworkers[158] prepared MOF thin films for electrochemical reduction of CO_2. The catalytic current density increased upon adjusting the thickness of the cobalt–porphyrin MOF films from 10 nm to 70 nm, and this effect was ascribed to increased cobalt loading within the sample. By monitoring CO and H_2 production, current selectivity for CO formation reached 76% at 0.7 V *vs.* RHE (Fig. 9). Farha and Hupp *et al.*[159] also reported robust MOF thin films for CO_2 reduction using the MOF-525 iron–porphyrin framework.

Hybrid catalytic materials are also of great interest. Zhao *et al.*[131] prepared Cu-MOF nanosheet composites with Au nanoparticles decorating the MOF surface. The catalytic

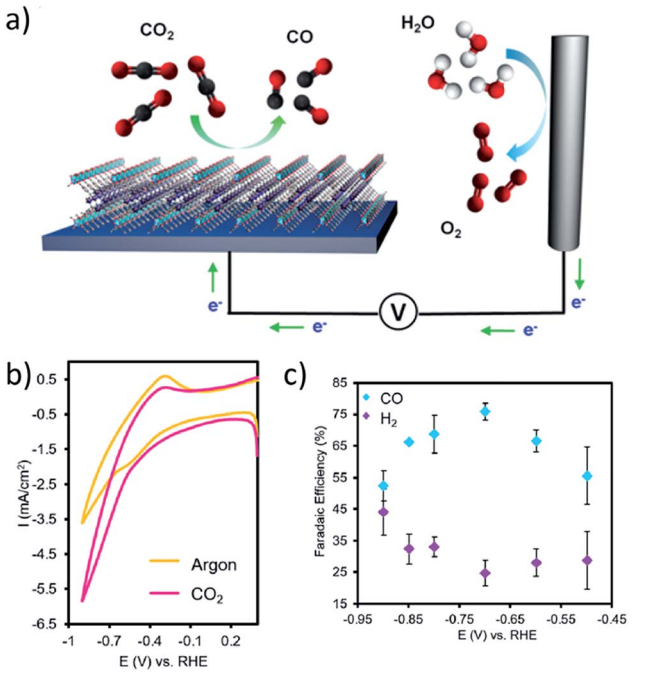

Fig. 9 (a) Schematic showing a thin film cobalt–porphyrin MOF, $Al_2(OH)_2$TCPP-Co, performing CO_2 reduction. (b) An increase in current is observed in the cyclic voltammogram when the MOF is subjected to a CO_2 environment. (c) Selectivity for generation of CO and H_2 was tested over the potential range −0.5 to −0.9 V *vs.* RHE with a reported peak faradaic efficiency for CO of 76%. Adapted with permission.[158] Copyright 2015 American Chemical Society.

behavior of the nanocomposite was investigated by monitoring reduction of 4-nitrophenol to 4-aminophenol by UV-vis absorption spectroscopy. The authors proposed that the layered MOF nanosheet architecture facilitates π–π stacking interactions between the MOF linker molecules and aromatic phenols. These interactions in turn improve electron transfer between the supported Au nanocatalysts and the phenol species. Zhang *et al.*[160] also prepared composites comprised of Au nanoparticles and MOF nanosheets. Their Au NP/CuTCPP(Co) hybrid material oxidized 3,3′,5,5′-tetramethylbenzidine in the presence of hydrogen peroxide and was considered to behave as a peroxidase biomimetic catalyst. Showing the potential benefit of mixing discrete MOF phases for catalytic effect, Dou *et al.*[161] incorporated Fe-MOF nanoparticles within Ni-MOF nanosheets and lowered the overpotential for OER to 256 mV, down from 370 mV for the neat Ni-MOF.

4.2 Charge transport and storage

The prospect of eliciting efficient and tunable charge transport and storage in 2D MOFs and COFs has driven extensive research over the past decade.[16,17,45,162–165] Multiple groups have developed graphene-like MOFs and COFs in hopes of achieving record values for conductivity or capacitance.[166–169] Dincă *et al.* produced one of the most highly conductive MOFs, $Ni_3(HITP)_2$, and subsequently prepared films with 500 nm thicknesses. Films deposited on quartz substrates resulted in room temperature conductivities of 40 S cm^{-1} and also exhibited higher conductivities with increasing temperature (Fig. 10).[168] Cánovas *et al.*[170] identified a 2D MOF, $Fe_3(THT)_2(NH_4)_3$, with a room temperature carrier mobility of 220 cm^2 V^{-1} s^{-1} and a direct bandgap of 0.25 eV. These semiconducting films were prepared by an interfacial growth method that yielded large area, multilayer samples.

Gómez-García and coworkers[56] further characterized both of their mixed-valence, magnetic Fe(II)/Fe(III) MOFs and reported room temperature conductivities of 0.03 and 0.003 S cm^{-1} for bulk crystals when measured parallel to the honeycomb MOF structure. Their measurements revealed much lower conductivities ($\sim 10^{-4}$ and 10^{-6} S cm^{-1}) when measuring perpendicular to the honeycomb layer. Though nanosheets of these MOFs were produced, their associated carrier conductivities were not reported. Conversely, Nishihara *et al.*[142] successfully prepared nanosheets of their nickel bis(dithiolene) complex and reported a conductivity of 160 S cm^{-1} for a single crystalline flake using a four-point probe setup within an SEM. Also using four-point probe measurements, Zhu *et al.*[70] recorded a high conductivity of 1580 S cm^{-1} for their copper benzenehexathiol (Cu-BHT) coordination polymer. FETs were subsequently prepared from the Cu-BHT films and exhibited high hole- and electron-mobilities, with a single FET device managing to exhibit a hole mobility of 99 cm^2 V^{-1} s^{-1} and electron mobility of 116 cm^2 V^{-1} s^{-1}. Xu *et al.*[171] also fabricated a FET incorporating a $Ni_3(HITP)_2$ membrane prepared *via* an air–liquid interfacial method. Multiple devices indicated hole mobilities ranging from 38 ± 8 cm^2 V^{-1} s^{-1} to 48.6 cm^2 V^{-1} s^{-1}. The authors

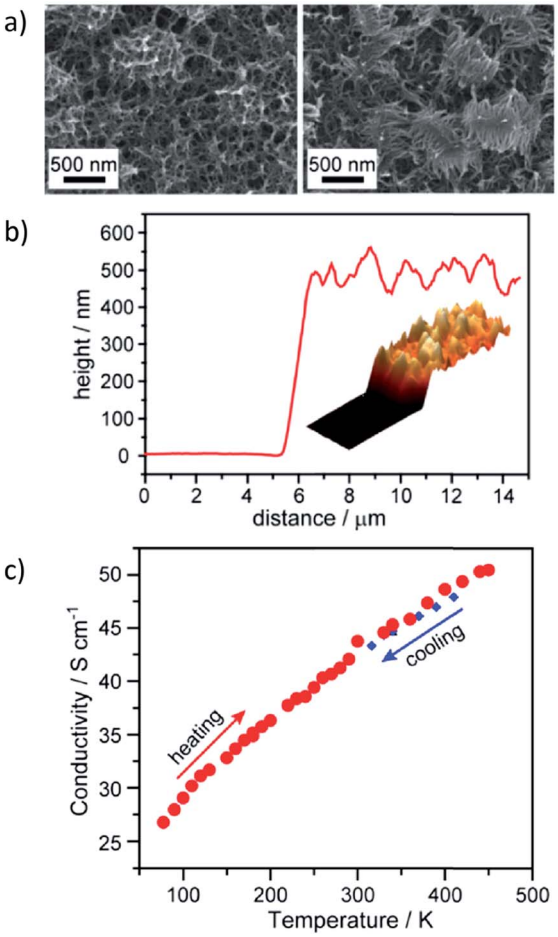

Fig. 10 a) SEM micrographs of $Ni_3(HITP)_2$ films with 500 nm thickness measured *via* (b) AFM. (c) van der Pauw conductivity measurements at various temperatures show reversible increase in conductivity for 500 nm thick films on quartz. Adapted with permission.[168] Copyright 2014 American Chemical Society.

hypothesized that these high values result from extensive charge delocalization within the layers, which are comprised of nickel ions coordinated to ligands with radical character. Close-packing of each vertical layer may also introduce opportunistic π–π interactions.

Pursuing the goal of targeted molecular design of graphene-like MOFs and COFs, Dichtel *et al.* prepared oriented thin films of a COF comprised of a redox-active monomer, 2,6-diaminoanthraquinone (DAAQ), and 1,3,5-triformylphluroglucinol (TFP).[172] Slow injection of TFP into a DAAQ solution yields 60–560 nm thick oriented thin films with areal capacitance values from 1.2 to 3.0 mF cm^{-2} that are higher than those measured on randomly oriented slurries, thereby suggesting the supercapacitor potential of the former. Over 5000 galvanostatic charge–discharge cycles (GCDC), the films show only 7% capacitance loss. Focusing on their $Ni_3(HITP)_2$ material, Dincă *et al.* prepared the first solely MOF comprised electrochemical double layer capacitors (EDLCs) and showed that their devices reach a normalized gravimetric capacitance of 18 μF cm^{-2}, exceeding the values observed in most carbon materials.[173]

Additional studies have also utilized exfoliated COF nanosheets and films as ion conductors and charge storage materials.[63,64,174–176] Chen *et al.* prepared a cationic COF skeleton nanosheet to sequester lithium salt anions and increase the concentration of free Li^+, and in so doing increased lithium conductivity within the material.[174] Furthermore, Fan and coworkers recently showed an ~3-fold increase in the specific capacitance of CTF-1 triazine COF nanosheets, relative to the bulk COF, and also noted improved capacity retention during cycling of lithium batteries wherein CTF-1 was used as the anode material.[64] These results collectively encourage continued efforts to demonstrate the unique potential of MOFs and COFs as active components in charge carrying and storing devices.

Surface-mounted MOF (SURMOF) or COF thin films and 2D sheets can serve as prototypical examples of organized molecular systems for device applications. Ballav *et al.* prepared a Cu-TCNQ SURMOF on mercaptoundecoanoic acid-functionalized FTO and Au substrates using the layer-by-layer (LbL) method.[177] Electron beam lithography facilitated the fabrication of Cu-TCNQ SURMOF thin film devices with consistent conductivity values in the range of 10^{-5} S cm^{-1}. The SURMOF of Cu-TCNQ also exhibited unique rectifying behavior when exposed to I_2 vapor, while bulk Cu-TCNQ under identical exposure conditions did not. Though not explicitly a SURMOF, Allendorf *et al.*[88] prepared a $Cu_3(BTC)_2$ thin film on patterned SiO_2/Si wafers and soaked the film in a TCNQ/dichloromethane solution to load the MOF with conductive TCNQ. The conductivity of the loaded film was measured to be as high as 7 S m^{-1}, thereby suggesting that loading 2D molecular materials with functional compounds may likewise be a viable strategy for introducing desirable properties.

4.3 Sensing

Two-dimensional MOFs and COFs are attractive candidate sensor materials due to their highly exposed pore and surface areas and the inherent sensitivity of their electronic structures to gating through adsorption or binding of analytes. MOF and COF thin film or nearly-2D materials have the potential to detect gases, solvents, metal ions[178,179] and contaminants[20,180] if interaction of these analytes with the framework induces, ideally reversible, optical, electronic, or crystallographic changes. In this regard, the Mirica group has recently demonstrated the broad utility of MOFs as sensors by incorporating assorted 2D frameworks into detection platforms. Their self-organized frameworks on textile (SOFT) devices (Fig. 11),[181] MOF-loaded shrinkable polymer films,[182] and bimetallic 2D MOF device prepared through dropcast[183] are good sensors for NO, H_2S, NH_3, and/or H_2O.

Focusing on smaller scale materials, Allendorf *et al.* prepared HKUST-1 thin films on substrates by spin coating a DMSO solution containing $Cu(NO_3)_2 \cdot 3H_2O$ and 1,3,5-benzenetricarboxylic acid in a layer-by-layer manner.[184] Between each layering cycle, the deposited HKUST-1 layer was heated for five minutes at 70 °C. As a final step, the MOF was soaked in methanol and activated at 100 °C for 30 min to ready the thin film for sensing tests (Fig. 12a). The purple films were exposed to 0.2–95% relative humidity (RH) at 296 K and reflectance spectroscopy was used to monitor the thin film response. Exposure to humidity, particularly at lower RH, red shifts the reflectance spectrum and correlates to a color change from purple to light blue in the HKUST-1 thin film. Removal of water through a 5 min dry air purge results in reversion of the MOF thin film to its previous state. In this manner, trends in the percent reflectance of the thin film as a function of RH were

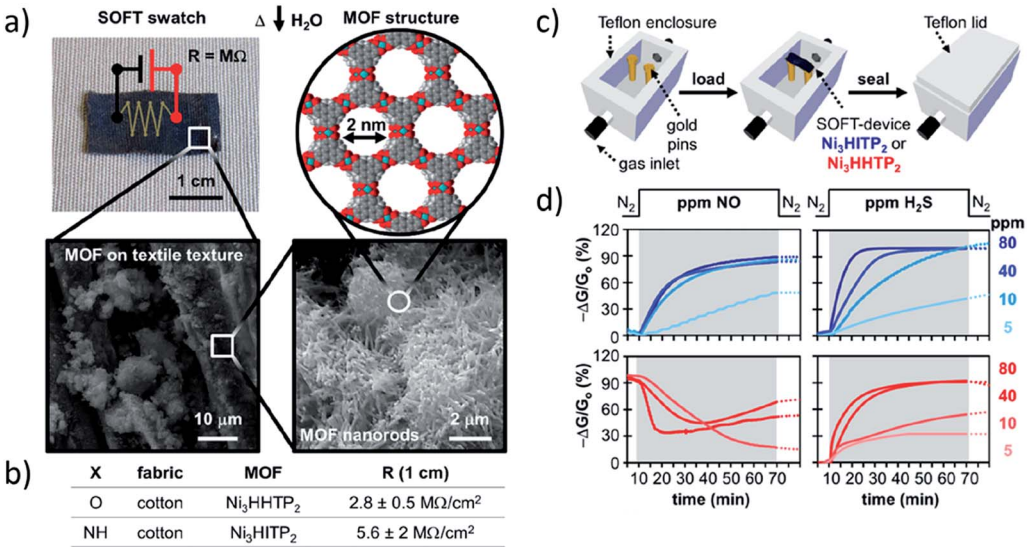

b) X	fabric	MOF	R (1 cm)
O	cotton	Ni_3HHTP_2	2.8 ± 0.5 MΩ/cm²
NH	cotton	Ni_3HITP_2	5.6 ± 2 MΩ/cm²

Fig. 11 (a) Conductive SOFT-devices produced from solvothermal condensation of MOF reagents in water onto textiles. Photograph of SOFT-device (top left), SEM images of textile fibers coated by MOF film (bottom left), SEM image of characteristic MOF nanorod structure (bottom right), and space-filling model of MOF (top right). (b) Sheet resistance measurements for SOFT-devices. (c) Schematic of custom enclosure for measuring (d) response of SOFT-sensors when exposed to NO (left) or H_2S (right). Adapted with permission.[181] Copyright 2017 American Chemical Society.

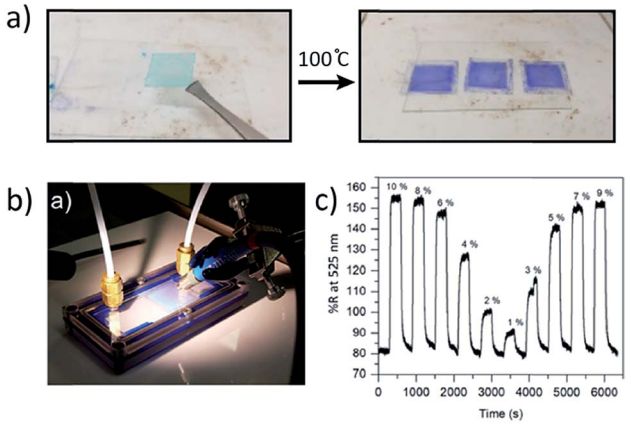

Fig. 12 (a) Color change from blue to purple upon activation of the HKUST-1 thin films, which were deposited through layer-by-layer methods. (b) Photograph of the authors' gas flow cell and reflectance measurement setup. (c) Plot of percent reflectance *vs.* time of HKUST-1 thin films upon their exposure to 0–10% RH for 5 min, followed by 5 min intervals of dry air purge. Adapted with permission.[184] Copyright 2018 American Chemical Society.

assessed (Fig. 12b and c). The thin film was even incorporated into a practical LED photodector for low RH testing. Eddaoudi *et al.* prepared two thin films, NbOFFIVE-1-Ni and ALFFIVE-1-Ni, that enabled detection of CO_2 down to 400–5000 ppm.[185] In this work, a novel paste-like MOF deposition method was used to prepare homogenous and uniform thin film coatings of both MOFs on interdigitated electrodes (IDE) and QCMs. The IDE sensing assessment showed a decrease in capacitance of the MOFs during their exposure to various CO_2 concentrations, while QCM data reflected *in situ* changes in the MOFs' mass due to surface adsorption of CO_2.

Many MOF or COF thin films have been prepared to detect small organic molecules. Dincă *et al.* dropcasted $Cu_3(HITP)_2$ [186] dispersions to prepare an ammonia vapor sensor with sub-ppm detection capabilities. Xu *et al.*[141] demonstrated a 2–20 nm $Cu_3(HHTP)_2$ thin film grown by spray LbL as an excellent room-temperature, chemiresistive ammonia sensor. The thin film selectively detects ammonia and can reliably report on concentrations as low as 100 ppm. Dincă *et al.* also identified that pellets of their conductive 2D MOFs can be used as sensors for assorted volatile organic compounds,[13] suggesting that singly crystalline thin films or nanosheets could be promising sensors. Ethylamine sensing was accomplished by $Zn(BDC)(H_2O)$ MOF nanosheets prepared by Jiang *et al.*[187] Here, binding of ethylamine by the MOF was monitored through fluorescence spectroscopy. Banerjee and coworkers[36] identified COF nanosheets which exhibit a concentration-dependent fluorescence response in the presence of assorted nitroaromatic compounds such as 2,4,6-trinitrophenol (TNP). Xian *et al.* also reported on the use of covalent organic nanosheets as fluorescent sensors for TNP detection.[188] Sonication of their bulk polyimide COF produced nanosheets as thin as 1 nm, which amounts to only a few molecular layers. In the presence of increasing concentrations of TNP, the fluorescence intensity of the COF nanosheets decreased in a linear fashion. The authors suggest that this observed fluorescence quenching arises from ground state electron transfer from TNP^- to the COF framework. Liu *et al.*[117] prepared few-layer Zn-TCPP(BP) crystals by incorporating a 4,4′-biphenyldicarboxylic acid (BP) nucleation modulator during the growth process. The resulting zinc nanodisks catalytically bind then oxidize nitrite ions, exhibiting a low nitrite detection limit of 0.26 μM, owing to the large contact area and layered structure of crystalline Zn-TCPP(BP).

Biologically-inspired MOF sensors are also the focus of considerable research into applications of MOF thin films and nanosheets. Electrochemical glucose detection was reported by Lu and Wu[125] with their nickel-based MOF nanosheet on nickel foam. The Ni-MOF/nickel foam electrode exhibited a unique oxidation peak in CV measurements compared to a bare nickel foam electrode. The magnitude of this oxidation peak was enhanced upon addition of a 1.0 mM glucose solution, possibly due to catalytic oxidation of glucose to gluconolactone by the Ni-MOF. Ultimately, the sensor exhibited a low 85 nM detection limit for glucose and a sensitivity of 14 858 μA mM^{-1} cm^{-2}. Ultrathin imine-linked COF nanosheets, TPA-COF, prepared by Zhang and coworkers were used for DNA detection.[189] Solutions of TPA-COF nanosheets were added to mixtures of buffer containing hairpin DNA probes, H1 (fluorescent dye-labeled) and H2. H1 individually interacts with TPA-COF nanosheets and is quenched due to π–π interactions. In the presence of target DNA, a hybridization chain reaction occurs and forms double-stranded DNA (dsDNA). In this case, H1 no longer interacts with TPA-COF nanosheets and fluorescence is recovered. The authors noted that the magnitude of fluorescence quenching is enhanced when nanosheets of TPA-COF are used instead of the bulk COF. Zhang *et al.* reported similar DNA sensing experiments for their surfactant-formed MOF nanosheets.[77] Other nanoscale MOF sensors have been used to detect intracellular pH[190] and O_2 [191] or have served as electrochemical H_2O_2 sensors.[192]

4.4 Separations

The pore size and functionality of 2D MOF and COF materials[193] can be designed to host specific chemical interactions and to impose specific constraints ideally suited for selective gas[194,195] and liquid separation,[196–199] enantiomer separation,[200–202] and even targeted drug delivery.[27] Liquid separations are commonly modeled with dye molecules and have been pursued with MOF and COF membranes. Ang and Hong prepared porphyrin-based Zn-TCP(Fe) nanosheets with carboxylate pendant groups at the nanosheet edges, which cross-link with polycationic polymer molecules.[203] The nanosheets were then transferred to nylon supports. The 48 nm membranes exhibit minimal defects and high water permeance. Impressive rejection rates for four organic dyes, methyl red (MR), methylene blue (MnB), methyl orange (MO), and brilliant blue G (BB), and four salts, $MgCl_2$, Na_2SO_4, NaCl, and $MgSO_4$ were determined. Banerjee *et al.* prepared self-standing covalent organic membranes[204] comprised of platelet-like COF sheets. Though the membranes themselves are thick, 200–700 μm, separation of rose Bengal (RB), methylene blue (MB) and Congo red (CR) aqueous dye solutions was successful, with demonstrated rejection rates of

99%, 96% and 94%, respectively. Active pharmaceutical ingredients (APIs) such as vitamin B12 and tetracycline were rejected at rates as high as 99% and 81%. Such membranes may serve as an affordable and robust solution to current wastewater treatment concerns. Additional work by Banerjee and coworkers[205] prepared large area, transparent COF thin films with thicknesses of 50–90 nm from liquid–liquid interfacial synthesis. Rejection rates for an additional set of organic dyes were calculated between 79–99% for these films. Furthermore, the films appeared stable during at least 24 hour periods of continuous aqueous solution exposure. In an alternative application of liquid separations, MOFs and COFs have been targeted as potential materials for water desalination. Grossman *et al.* previously showed nanoporous graphene was effective at filtering NaCl salt from water[206] and expanded their efforts to COFs.[207] In a computational investigation, ultrathin films of a 2D triazine COF were assessed and found to reject salt at a 91% rate while allowing water to pass through at a rate of 70 L per cm^2 per day per MPa. Calculations have also shown that COF nanosheets can in principle reject 100% of $MgCl_2$ with high waterpermeance.[208] Other computational efforts have considered the incorporation of UiO-66 MOFs in membranes for desalination,[209] with a recent study by Zhao *et al.* showing Na^+ rejection as high as 74.9% with fair aqueous stability.[210] Continued improvement of COF and MOF aqueous stabilities is required before their potential in water desalination is fully realized.

With regards to gas separations, Zhao *et al.*[211] prepared ~4 nm thick nanosheets from their nickel based MAMS-1 MOF by gentle freeze-thaw exfoliation, which was used to avoid extensive crystal damage. Subsequent hot-drop casting deposited aligned nanosheets onto anodic aluminum oxide substrates. The resulting membranes (which ranged 4–40 nm in thickness) exhibited thermo-switchable H_2 permeation and impressive H_2/CO_2 separation for 2D membranes. Dam and coworkers[212] prepared a MOF thin film on the surface of a Pd thin film to serve as a protective, pre-sieving layer for CO/H_2 separation. Long *et al.*[213] prepared a mixed-matrix membrane loaded with Mg_2(dobdc) MOF nanocrystals. Polymer films loaded with MOF nanocrystals exhibited increased gas permeability for H_2, N_2, CH_4, and CO_2 and improved separation of H_2/CH_4 and H_2/N_2 mixtures. COFs have also been integrated into mixed-matrix membranes for gas separations applications. Zhao *et al.* exfoliated bulk, water-stable COFs into monolayers or nanosheets which were subsequently mixed with poly(ether imide) or polybenzimidazole. Their NUS-2@PBI membrane, loaded with 20% COF, showed a 31.4H_2/CO_2 selectivity.[214] Other mixed-matrix membranes prepared with COF-5 nanosheets and Pebax-1657 show high CO_2 uptake capacities and 49.3 CO_2/N_2 selectivity compared to the neat polymer membrane. These results were accomplished with a COF loading as low as 0.4 wt%.[215]

4.5 Gas uptake

The same features that enable MOF and COF thin films to participate in selective molecular separations render them promising candidates as gas storage materials. Carbon dioxide storage has attracted much attention from the MOF and COF community but remains challenging for MOF and COF nanosheets, which lack bulk porosity for adsorption. Moorthy *et al.*[216] delaminated their bulk imidazole and triptycene-based MOFs into nanosheets by disrupting interlayer hydrogen bonding. CO_2 adsorption capacities as high as 124–208 $cm^3\ g^{-1}$ were measured for the bulk MOFs and are better than reported uptake values for N_2 and H_2, but adsorption capacities are not reported for the nanosheets. Do *et al.*[217] formed nanocube, nanosheet, and nanorod morphologies of their $Cu_2(ndc)_2$(dabco) MOF by incorporating acetic acid and/or pyridine modulators during synthesis. CO_2 uptake for each morphology was improved relative to the bulk, and measured 5.0, 4.8, 4.3, and 3.5 mmol g^{-1} (at 1 bar and 273 K) for the nanocube, nanosheet, nanorod, and bulk samples, respectively. By modulating crystal growth and repressing certain crystal faces, tailored materials with specific morphologies and facial functionalities can be prepared. Kang and coworkers[218] compared CO_2 working capacities of ZIF-8, ZIF-L, and dia(Zn)-HCOONa (a hexagonal nanosheet). At elevated temperatures between 50–100 °C, similar working capacities were observed whereas the latter two systems were considered nonporous at 77 K in N_2 physisorption experiments. The authors suggest increased framework flexibility at higher temperatures likely correlates to increased CO_2 adsorption. Coskun *et al.* synthesized graphene/ZIF-8 composites[219] and investigated their CO_2 capture at 303 K and at pressures as high as 35 bar. Rao *et al.*[220] also prepared graphene/MOF composites with their Cd-PBM MOF. The composites, totaling 2.5–3 nm in thickness, appear to undergo uptake of CO_2 in a stepwise manner with significant hysteresis. In efforts to improve MOF gas adsorption on the nanoscale, Zhang and coworkers demonstrated higher CO_2 uptake by ZIF-L nanosheets supported on halloysite nanotube (HNT) membranes compared to samples without HNT.[221] Careful selection of substrates and solid supports are therefore crucial in continued understanding of nanosheet properties.

4.6 Protective coatings

The chemical resilience of many MOF and COF thin films and 2D molecular materials has motivated their use as protective coatings for assorted functional materials.[95,222] Multiple biological applications of MOF coatings have been pursued. Falcaro *et al.*[223] crystallized a ZIF-8 film on the surface of a β-galactosidase-coated eukaryotic yeast cell. The ~100 nm MOF film protected the cell from toxic compounds and still allowed for diffusion of important bioactive molecules such as lactose. Interestingly, the cells were able to resume normal growth upon removal of the MOF. Wöll *et al.*[224] demonstrated two potential SURMOF thin film coatings that were highly stable in water and artificial seawater and were harmless to surrounding fibroblasts, which were used to model a cellular environment. Tsotsalas *et al.*[225] utilized a SURMOF film coating as an intermediate on pathway to a porphyrin polymer thin film. The film demonstrated antibacterial activity toward *E. coli* in the presence of light, indicating that $^1O_2$ and free radicals likely

contributed to bacterial death. Wöll and coworkers also demonstrated the ability to convert SURMOFs to gel coatings.[225] In a demonstration of the potential for MOFs to serve as defensive coatings against chemical warfare agents, Farha *et al.*[226] showed that thin films of assorted zirconium metal–organic frameworks were able to photocatalytically oxidize 2-chloroethyl ethyl sulfide (CEES), a mustard gas simulant. Thin films of MOFs UMCM-313 and NU-1000 were prepared on FTO substrates using a LbL technique. Irradiation of the thin films by LEDs produced singlet oxygen, which was responsible for oxidizing the mustard gas simulant to nontoxic products with CEES half-lives of 145 min and 76 min (Fig. 13). Ultimately, the thin films showed a higher TOF than the bulk MOFs. Other studies have shown MOF thin films can also be used as functional coatings for microelectrodes in electrocatalytic reactions such as CO_2 reduction.[227]

5. Prospects for future research

The future is bright for 2D molecular materials especially if breakthroughs in the synthesis, characterization, and utilization of these materials can mirror the great research strides made in 2D atomic materials over the past decade. 2D molecular frameworks allow for an exceptional degree of freedom in chemical design, a feature that bodes well for uncovering a plethora of new properties and applications. By drawing upon synthetic and analytical expertise from the chemical (*e.g.* inorganic and physical), physical (*e.g.* condensed matter), and engineering communities, 2D molecular materials research has the potential to spawn new interdisciplinary research collaborations. Ultimately, 2D molecular lattices, be they 2D MOFs or COFs, are a compelling platform through which to discover new and emergent properties and to expand the library of 2D materials.

Several areas of research should be prioritized to fulfill the myriad opportunities presented by 2D molecular lattices. First, synthetic breakthroughs are needed to consistently prepare high-quality MOF and COF thin films and true 2D lattices. Explicit control of dimensionality and phase is vital, as is attention to preparing these defect-free materials at scale for integration into technology platforms. In this regard, gas-phase methods show promise and need further investigation. Second, characterization techniques capable of high-throughput and *in situ* analysis are desirable. The often tedious, but necessary, process of characterizing in detail discrete 2D nanosheets or discrete regions of larger samples would benefit from automated methods or faster screening methods. Likewise, continued development of *in situ* characterization techniques for 2D molecular materials is crucial to advance investigation of these systems. Scanning tunneling microscopy/spectroscopy (STM/S) could emerge as a powerful technique for visualizing the structural and electronic evolution of single MOF or COF layers as they are assembled on surfaces. Finally, rigorous electronic transport measurements performed on devices fabricated from crystalline 2D molecular lattices and thin films are a vital tool for uncovering new physics and new opportunities to create optoelectronic devices. The aforementioned efforts must be pursued alongside existing studies exploring the potential of true 2D MOFs and COFs for electronics, energy storage, catalysis, and biomedicine.

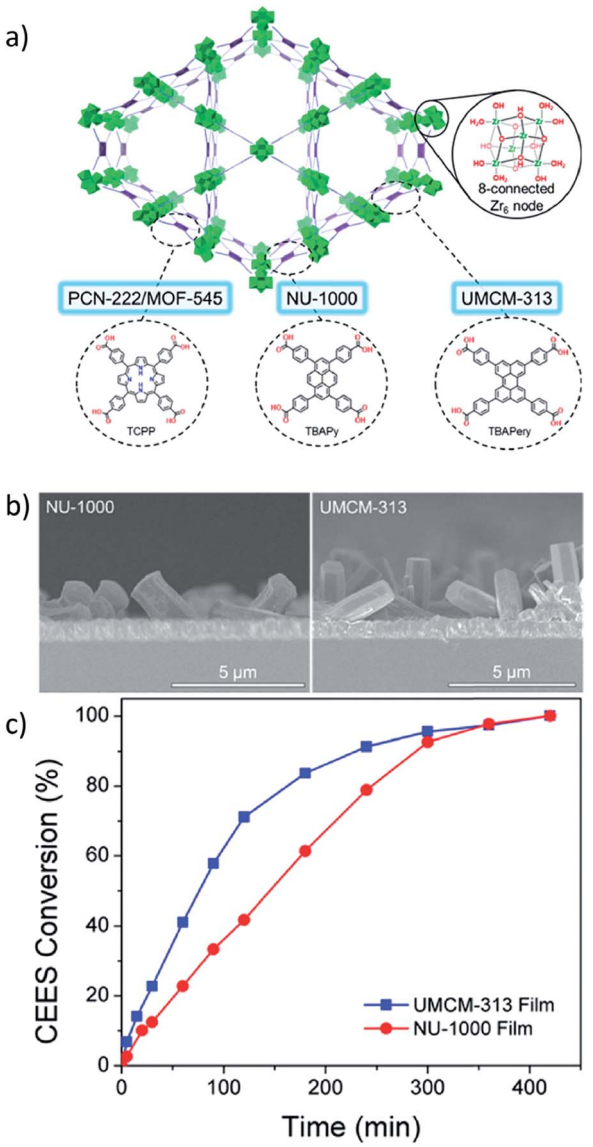

Fig. 13 (a) General structure of three MOFs, PCN-222/MOF-545, NU-1000, and UMCM-313, used as a thin-film protective coating against mustard gas simulant. (b) NU-1000 and UMCM-313 thin films prepared using layer-by-layer techniques on FTO substrates and (c) their reaction profiles for the photocatalytic oxidation of CEES. Adapted with permission.[226] Copyright 2018 American Chemical Society.

Abbreviations

$Zn_2(bim)_4$	Poly[Zn_2(benzimidazole)$_4$]
PPF-1	Zn_2(tetrakis(4-carboxyphenyl)porphyrin)$_4$
$Cu_2(bdc)_2$, Cu(bdc)	Cu_2(1,4-benzenedicarboxylate)$_2$
Cu(BHT)	Cu_3(benzenehexathiol)$_n$
$Au_3(BHT)_2$	Au_3(benzenehexathiol)$_2$

$Ag_3(BHT)_2$	Ag_3(benzenehexathiol)$_2$
Zn-TCPP (*i.e.*, PPF-1)	Zn_2(tetrakis(4-carboxyphenyl)porphyrin)$_4$
Zn(Bim)OAc	Zn(benzimidazole)(acetate)
Cu-TCPP	Cu_2(tetrakis(4-carboxyphenyl)porphyrin)$_4$
CoTCPP	5,10,15,20-Tetrakis(4-carboxyphenyl) porphyrinato-cobalt(II)
ZIF-8	Zn(2-methylimidazolate)$_2$
HKUST-1	Cu_3(1,3,5-benzenetricarboxylate)$_2$
Cu_3HTTP_2	Cu-2,3,6,7,19,11-hexahydroxy-triphenylene
COF-5	$C_9H_4BO_2$, from 1,4-phenylene-bis(boronic acid) (PBBA) and 2,3,6,7,10,11-hexahydroxy-triphenylene (HHTP)
LZU-1	$(C_6H_4N)_n$, from 1,3,5-triformylbenzene and 1,4-diaminobenzene
MOF-5	Zn_4O(1,4-benzenedicarboxylate)$_3$
UiO-66	$Zr_6O_4(OH)_4$(1,4-benzenedicarboxylate)$_6$
MF-ZrBTB	$[Zr_6O_4(OH)_4]_6$[1,3,5-tris(4-carboxyphenyl) benzene acid]$_3$
Cu-BTC (HKUST-1)	Cu_3(1,3,5-benzenetricarboxylate)$_2$
Ni-BHT	Ni-benzenhexathiolate
Fe-BHT	Fe-benzenhexathiolate
Co-BHT	Co-benzenhexathiolate
NiIT	Bis(1-iminobenzene-2-thiolato)nickel(II)
Co-BDC	Co-1,4-benzenedicarboxylate
$Ni_3(HITP)_2$	Ni_3(2,3,6,7,10,11-hexaiminotriphenylene)$_2$
MOF-525	$Zr_6O_4(OH)_4(TpCPP\text{-}H_2)_3$
$Fe_3(THT)_2(NH_4)_3$	Fe_3(THT, 2,3,6,7,10,11-triphenylenehexathiol)$_2(NH_4)_3$
Cu-BHT	Cu-benzenhexathiolate
Cu-TCNQ	Cu-tetracyanoquinodimethane
NbOFFIVE-1-Ni	$[NbOF_5]^{2-}$ and Ni(pyrazine)$_2$
ALFFIVE-1-Ni	$AlF_5(H_2O)]^{2-}$ and Ni(pyrazine)$_2$
$Cu_3(HHTP)_2$	Cu_3(2,3,6,7,10,11-hexahydroxytriphenylene)$_2$
Zn(BDC)H_2O	Zn-1,4-benzenedicarboxylate
TPA-COF	[3+3] imine-linked COF prepared from tris(4-aminophenyl)amine and tris(4-formylphenyl)amine
MAMS-1	Ni_8(5-*tert*-butyl-1,3-benzenedicarboxylic acid)$_6$(μ-OH)$_4$)
Mg_2(dobdc)	Mg_2(2,5-dioxido-1,4-benzenedicarboxylate)
$Cu_2(ndc)_2$(dabco)	Cu_2(1,4-naphthalene dicarboxylate)2(1,4-diazabicyclo[2.2.2]-octane)
ZIF-L	Polymorph of ZIF-8, Zn(2-methylimidazolate)$_2$
diaz(Zn)-HCOONa	Polymorph of ZIF-8, Zn(2-methylimidazolate)$_2$
Cd-PBM	$\{Cd_4$(4,4′-azopyridine)$_2$(pyridine-2,3-dicarboxylate)$_4(H_2O)_2 \cdot 9H_2O\}_n$
UMCM-313	Zr_6 node and 2,5,8,11-tetrakis(4-carboxyphenyl)perylene
NU-1000	Zr_6 node and 1,3,6,8-tetrakis(*p*-benzoate) pyrene

Conflicts of interest

There are no conflicts of interest to declare.

References

1 C. Tan, X. Cao, X. J. Wu, Q. He, J. Yang, X. Zhang, J. Chen, W. Zhao, S. Han, G. H. Nam, M. Sindoro and H. Zhang, Recent Advances in Ultrathin Two-Dimensional Nanomaterials, *Chem. Rev.*, 2017, **117**, 6225–6331.
2 P. Miró, M. Audiffred and T. Heine, An atlas of two-dimensional materials, *Chem. Soc. Rev.*, 2014, **43**, 6537–6554.
3 D. L. Duong, S. J. Yun and Y. H. Lee, van der Waals Layered Materials: Opportunities and Challenges, *ACS Nano*, 2017, **11**, 11803–11830.
4 G. R. Bhimanapati, Z. Lin, V. Meunier, Y. Jung, J. Cha, S. Das, D. Xiao, Y. Son, M. S. Strano, V. R. Cooper, L. Liang, S. G. Louie, E. Ringe, W. Zhou, S. S. Kim, R. R. Naik, B. G. Sumpter, H. Terrones, F. Xia, *et al.*, Recent Advances in Two-Dimensional Materials beyond Graphene, *ACS Nano*, 2015, **9**, 11509–11539.
5 K. S. Novoselov, A. Mishchenko, A. Carvalho and A. H. Castro Neto, 2D materials and van der Waals heterostructures, *Science*, 2016, **353**, aac9439.
6 Z. Meng, R. M. Stolz, L. Mendecki and K. A. Mirica, Electrically-transduced chemical sensors based on two-dimensional nanomaterials, *Chem. Rev.*, 2019, **119**, 478–598.
7 A. J. Mannix, B. Kiraly, M. C. Hersam and N. P. Guisinger, Synthesis and chemistry of elemental 2D materials, *Nat. Rev. Chem.*, 2017, **1**, 1–15.
8 A. K. Geim and I. V. Grigorieva, van der Waals heterostructures, *Nature*, 2013, **499**, 419–425.
9 N. Huang, P. Wang and D. Jiang, Covalent organic frameworks: a materials platform for structural and functional designs, *Nat. Rev. Mater.*, 2016, **1**, 1–19.
10 S. Y. Ding and W. Wang, Covalent organic frameworks (COFs): from design to applications, *Chem. Soc. Rev.*, 2013, **42**, 548–568.
11 H. Furukawa, K. E. Cordova, M. O'Keeffe and O. M. Yaghi, The chemistry and applications of metal-organic frameworks, *Science*, 2013, **341**, 1230444.
12 B. Li, H. M. Wen, Y. Cui, W. Zhou, G. Qian and B. Chen, Emerging Multifunctional Metal–Organic Framework Materials, *Adv. Mater.*, 2016, **28**, 8819–8860.
13 M. G. Campbell, S. F. Liu, T. M. Swager and M. Dincă, Chemiresistive Sensor Arrays from Conductive 2D Metal-Organic Frameworks, *J. Am. Chem. Soc.*, 2015, **137**, 13780–13783.
14 S. Kitagawa, R. Kitaura and S. I. Noro, Functional porous coordination polymers, *Angew. Chem., Int. Ed.*, 2004, **43**, 2334–2375.
15 T. Islamoglu, S. Goswami, Z. Li, A. J. Howarth, O. K. Farha and J. T. Hupp, Postsynthetic Tuning of Metal-Organic Frameworks for Targeted Applications, *Acc. Chem. Res.*, 2017, **50**, 805–813.
16 W. Zheng, C. S. Tsang, L. Y. S. Lee and K. Y. Wong, Two-dimensional metal-organic framework and covalent-

organic framework: synthesis and their energy-related applications, *Mater. Today Chem.*, 2019, **12**, 34–60.
17 D. D. Medina, T. Sick and T. Bein, Photoactive and Conducting Covalent Organic Frameworks, *Adv. Energy Mater.*, 2017, **7**, 1–8.
18 L. E. Kreno, K. Leong, O. K. Farha, M. Allendorf, R. P. Van Duyne and J. T. Hupp, Metal-organic framework materials as chemical sensors, *Chem. Rev.*, 2012, **112**, 1105–1125.
19 Z. Y. Yeo, S. P. Chai, P. W. Zhu and A. R. Mohamed, An overview: synthesis of thin films/membranes of metal organic frameworks and its gas separation performances, *RSC Adv.*, 2014, **4**, 54322–54334.
20 X. Fang, B. Zong and S. Mao, Metal–Organic Framework-Based Sensors for Environmental Contaminant Sensing, *Nano-Micro Lett.*, 2018, **10**, 1–19.
21 L. Sun, M. G. Campbell and M. Dincă, Electrically Conductive Porous Metal-Organic Frameworks, *Angew. Chem., Int. Ed.*, 2016, **55**, 3566–3579.
22 H. Wang, Z. Zeng, P. Xu, L. Li, G. Zeng, R. Xiao, Z. Tang, D. Huang, L. Tang, C. Lai, D. Jiang, Y. Liu, H. Yi, L. Qin, S. Ye, X. Ren and W. Tang, Recent progress in covalent organic framework thin films: fabrications, applications and perspectives, *Chem. Soc. Rev.*, 2019, **48**, 488–516.
23 Y. Peng, Y. Li, Y. Ban, H. Jin, W. Jiao, Z. Liu and W. Yang, Metal-organic framework nanosheets as building blocks for molecular sieving membranes, *Science*, 2014, **346**, 1356–1359.
24 G. Lan, Z. Li, S. S. Veroneau, Y.-Y. Zhu, Z. Xu, C. Wang and W. Lin, Photosensitizing Metal–Organic Layers for Efficient Sunlight-Driven Carbon Dioxide Reduction, *J. Am. Chem. Soc.*, 2018, **140**, 12369–12373.
25 J. L. Segura, S. Royuela and M. Mar Ramos, Post-synthetic modification of covalent organic frameworks, *Chem. Soc. Rev.*, 2019, **48**, 3903–3945.
26 P. Samanta, A. V. Desai, B. Anothumakkool, M. M. Shirolkar, A. Karmakar, S. Kurungot and S. K. Ghosh, Enhanced proton conduction by post-synthetic covalent modification in a porous covalent framework, *J. Mater. Chem. A*, 2017, **5**, 13659–13664.
27 S. Mitra, H. S. Sasmal, T. Kundu, S. Kandambeth, K. Illath, D. Díaz Díaz and R. Banerjee, Targeted Drug Delivery in Covalent Organic Nanosheets (CONs) via Sequential Postsynthetic Modification, *J. Am. Chem. Soc.*, 2017, **139**, 4513–4520.
28 A. Schneemann, V. Bon, I. Schwedler, I. Senkovska, S. Kaskel and R. A. Fischer, Flexible metal–organic frameworks, *Chem. Soc. Rev.*, 2014, **43**, 6062–6096.
29 M. Zhao, Y. Huang, Y. Peng, Z. Huang, Q. Ma and H. Zhang, Two-dimensional metal-organic framework nanosheets: synthesis and applications, *Chem. Soc. Rev.*, 2018, **47**, 6267–6295.
30 V. Stavila, A. A. Talin and M. D. Allendorf, MOF-based electronic and opto-electronic devices, *Chem. Soc. Rev.*, 2014, **43**, 5994–6010.
31 S. Li, K. Yang, C. Tan, X. Huang, W. Huang and H. Zhang, Preparation and applications of novel composites composed of metal-organic frameworks and two-dimensional materials, *Chem. Commun.*, 2016, **52**, 1555–1562.
32 *Layered graphene*, available at, http://www.graphenomenon.com/.
33 N. Wang, *et al.*, *One-molecule-thick material has big advantages MIT News*, 2012, available at, https://http://news.mit.edu/2012/graphene-molybdenum-disulfide-flat-materials-0823.
34 F. J. Claire, S. M. Tenney, M. M. Li, M. A. Siegler, J. S. Wagner, A. S. Hall and T. J. Kempa, Hierarchically Ordered Two-Dimensional Coordination Polymers Assembled from Redox-Active Dimolybdenum Clusters, *J. Am. Chem. Soc.*, 2018, **140**, 10673–10676.
35 D. J. Ashworth and J. A. Foster, Metal-organic framework nanosheets (MONs): a new dimension in materials chemistry, *J. Mater. Chem. A*, 2018, **6**, 16292–16307.
36 G. Das, B. P. Biswal, S. Kandambeth, V. Venkatesh, G. Kaur, M. Addicoat, T. Heine, S. Verma and R. Banerjee, Chemical sensing in two dimensional porous covalent organic nanosheets, *Chem. Sci.*, 2015, **6**, 3931–3939.
37 J. Liu, H. Yu, L. Wang, Z. Deng, K. R. Naveed, A. Nazir and F. Haq, Two-dimensional metal-organic frameworks nanosheets: synthesis strategies and applications, *Inorg. Chim. Acta*, 2018, **483**, 550–564.
38 W. Liu, R. Yin, X. Xu, L. Zhang, W. Shi and X. Cao, Structural Engineering of Low-Dimensional Metal-Organic Frameworks: Synthesis, Properties, and Applications, *Adv. Sci.*, 2019, 1802373.
39 T. Kambe, R. Sakamoto, K. Hoshiko, K. Takada, M. Miyachi, J. H. Ryu, S. Sasaki, J. Kim, K. Nakazato, M. Takata and H. Nishihara, π-Conjugated nickel bis(dithiolene) complex nanosheet, *J. Am. Chem. Soc.*, 2013, **135**, 2462–2465.
40 R. Sakamoto, K. Takada, T. Pal, H. Maeda, T. Kambe and H. Nishihara, Coordination nanosheets (CONASHs): strategies, structures and functions, *Chem. Commun.*, 2017, **53**, 5781–5801.
41 I. Stassen, D. De Vos and R. Ameloot, Vapor-Phase Deposition and Modification of Metal–Organic Frameworks: State-of-the-Art and Future Directions, *Chem.–Eur. J.*, 2016, **22**, 14452–14460.
42 M. J. Cliffe, E. Castillo-Martínez, Y. Wu, J. Lee, A. C. Forse, F. C. N. Firth, P. Z. Moghadam, D. Fairen-Jimenez, M. W. Gaultois, J. A. Hill, O. V. Magdysyuk, B. Slater, A. L. Goodwin and C. P. Grey, Metal-Organic Nanosheets Formed via Defect-Mediated Transformation of a Hafnium Metal-Organic Framework, *J. Am. Chem. Soc.*, 2017, **139**, 5397–5404.
43 M. D. Allendorf, A. Schwartzberg, V. Stavila and A. A. Talin, A roadmap to implementing metal-organic frameworks in electronic devices: challenges and critical directions, *Chem.–Eur. J.*, 2011, **17**, 11372–11388.
44 J. Liu and C. Wöll, Surface-supported metal-organic framework thin films: fabrication methods, applications, and challenges, *Chem. Soc. Rev.*, 2017, **46**, 5730–5770.
45 M. Ko, L. Mendecki and K. A. Mirica, Conductive two-dimensional metal-organic frameworks as multifunctional materials, *Chem. Commun.*, 2018, **54**, 7873–7891.

46 L. Heinke and C. Wöll, Surface-Mounted Metal–Organic Frameworks: Crystalline and Porous Molecular Assemblies for Fundamental Insights and Advanced Applications, *Adv. Mater.*, 2019, 1806324.

47 M. Lischka, R. Dong, M. Wang, N. Martsinovich, M. Fritton, L. Grossmann, W. M. Heckl, X. Feng and M. Lackinger, Competitive Metal Coordination of Hexaaminotriphenylene on Cu(111) by Intrinsic Copper Versus Extrinsic Nickel Adatoms, *Chem.–Eur. J.*, 2019, **25**, 1975–1983.

48 S. Kim, H. Wang and Y. M. Lee, 2D Nanosheets and Their Composite Membranes for Water, Gas, and Ion Separation, *Angew. Chem., Int. Ed.*, 2019, **58**, 2–18.

49 C. Zhang, B.-H. Wu, M.-Q. Ma, Z. Wang and Z.-K. Xu, Ultrathin metal/covalent–organic framework membranes towards ultimate separation, *Chem. Soc. Rev.*, 2019, **48**, 3811–3841.

50 S. Yuan, X. Li, J. Zhu, G. Zhang, P. Van Puyvelde and B. Van Der Bruggen, Covalent organic frameworks for membrane separation, *Chem. Soc. Rev.*, 2019, **48**, 2665–2681.

51 E. Barankova, X. Tan, L. F. Villalobos, E. Litwiller and K. V. Peinemann, A Metal Chelating Porous Polymeric Support: The Missing Link for a Defect-Free Metal–Organic Framework Composite Membrane, *Angew. Chem., Int. Ed.*, 2017, **56**, 2965–2968.

52 M. Wu, H. Ye, F. Zhao and B. Zeng, High-quality metal-organic framework ZIF-8 membrane supported on electrodeposited ZnO/2-methylimidazole nanocomposite: efficient adsorbent for the enrichment of acidic drugs, *Sci. Rep.*, 2017, **7**, 1–9.

53 J. Sun, H. T. Kwon and H. K. Jeong, Continuous synthesis of high quality metal–organic framework HKUST-1 crystals and composites via aerosol-assisted synthesis, *Polyhedron*, 2018, **153**, 226–233.

54 L. M. Salonen, D. D. Medina, E. Carbó-Argibay, M. G. Goesten, L. Mafra, N. Guldris, J. M. Rotter, D. G. Stroppa and C. Rodríguez-Abreu, A supramolecular strategy based on molecular dipole moments for high-quality covalent organic frameworks, *Chem. Commun.*, 2016, **52**, 7986–7989.

55 M. Calik, T. Sick, M. Dogru, M. Döblinger, S. Datz, H. Budde, A. Hartschuh, F. Auras and T. Bein, From Highly Crystalline to Outer Surface-Functionalized Covalent Organic Frameworks-A Modulation Approach, *J. Am. Chem. Soc.*, 2016, **138**, 1234–1239.

56 S. Benmansour, A. Abhervé, P. Gómez-Claramunt, C. Vallés-García and C. J. Gómez-García, Nanosheets of Two-Dimensional Magnetic and Conducting Fe(II)/Fe(III) Mixed-Valence Metal-Organic Frameworks, *ACS Appl. Mater. Interfaces*, 2017, **9**, 26210–26218.

57 W. M. Liao, J. H. Zhang, S. Y. Yin, H. Lin, X. Zhang, J. Wang, H. P. Wang, K. Wu, Z. Wang, Y. N. Fan, M. Pan and C. Y. Su, Tailoring exciton and excimer emission in an exfoliated ultrathin 2D metal-organic framework, *Nat. Commun.*, 2018, **9**, 1–9.

58 Y. H. Luo, C. Chen, C. He, Y. Y. Zhu, D. L. Hong, X. T. He, P. J. An, H. S. Wu and B. W. Sun, Single-Layered Two-Dimensional Metal-Organic Framework Nanosheets as an in Situ Visual Test Paper for Solvents, *ACS Appl. Mater. Interfaces*, 2018, **10**, 28860–28867.

59 Y. Ding, Y. P. Chen, X. Zhang, L. Chen, Z. Dong, H. L. Jiang, H. Xu and H. C. Zhou, Controlled Intercalation and Chemical Exfoliation of Layered Metal-Organic Frameworks Using a Chemically Labile Intercalating Agent, *J. Am. Chem. Soc.*, 2017, **139**, 9136–9139.

60 J. Huang, Y. Li, R. K. Huang, C. T. He, L. Gong, Q. Hu, L. Wang, Y. T. Xu, X. Y. Tian, S. Y. Liu, Z. M. Ye, F. Wang, D. D. Zhou, W. X. Zhang and J. P. Zhang, Electrochemical Exfoliation of Pillared-Layer Metal–Organic Framework to Boost the Oxygen Evolution Reaction, *Angew. Chem., Int. Ed.*, 2018, **57**, 4632–4636.

61 C. Kutzscher, A. Gelbert, S. Ehrling, C. Schenk, I. Senkovska and S. Kaskel, Amine assisted top-down delamination of the two-dimensional metal-organic framework Cu2(bdc)2, *Dalton Trans.*, 2017, **46**, 16480–16484.

62 D. J. Ashworth, A. Cooper, M. Trueman, R. W. M. Al-Saedi, L. D. Smith, A. J. H. M. Meijer and J. A. Foster, Ultrasonic Exfoliation of Hydrophobic and Hydrophilic Metal–Organic Frameworks To Form Nanosheets, *Chem.–Eur. J.*, 2018, **24**, 17986–17996.

63 X. Chen, Y. Li, L. Wang, Y. Xu, A. Nie, Q. Li, F. Wu, W. Sun, X. Zhang, R. Vajtai, P. M. Ajayan, L. Chen and Y. Wang, High-Lithium-Affinity Chemically Exfoliated 2D Covalent Organic Frameworks, *Adv. Mater.*, 2019, **1–8**, 1901640.

64 Y. Zhu, X. Chen, Y. Cao, W. Peng, Y. Li, G. Zhang, F. Zhang and X. Fan, Reversible intercalation and exfoliation of layered covalent triazine frameworks for enhanced lithium ion storage, *Chem. Commun.*, 2019, **55**, 1434–1437.

65 P. Peng, L. Shi, F. Huo, S. Zhang, C. Mi, Y. Cheng and Z. Xiang, In Situ Charge Exfoliated Soluble Covalent Organic Framework Directly Used for Zn-Air Flow Battery, *ACS Nano*, 2019, **13**, 878–884.

66 M. A. Khayum, S. Kandambeth, S. Mitra, S. B. Nair, A. Das, S. S. Nagane, R. Mukherjee and R. Banerjee, Chemically Delaminated Free-Standing Ultrathin Covalent Organic Nanosheets, *Angew. Chem., Int. Ed.*, 2016, **55**, 15604–15608.

67 K. Yuan, T. Song, X. Zhu, B. Li, B. Han, L. Zheng, J. Li, X. Zhang and W. Hu, Construction of Large-Area Ultrathin Conductive Metal–Organic Framework Films through Vapor-Induced Conversion, *Small*, 2019, **15**, 1–6.

68 R. Dong, T. Zhang and X. Feng, Interface-Assisted Synthesis of 2D Materials: Trend and Challenges, *Chem. Rev.*, 2018, **118**, 6189–6325.

69 M. Shete, P. Kumar, J. E. Bachman, X. Ma, Z. P. Smith, W. Xu, K. A. Mkhoyan, J. R. Long and M. Tsapatsis, On the direct synthesis of Cu(BDC) MOF nanosheets and their performance in mixed matrix membranes, *J. Membr. Sci.*, 2018, **549**, 312–320.

70 X. Huang, P. Sheng, Z. Tu, F. Zhang, J. Wang, H. Geng, Y. Zou, C. A. Di, Y. Yi, Y. Sun, W. Xu and D. Zhu, A two-dimensional π-d conjugated coordination polymer with extremely high electrical conductivity and ambipolar transport behaviour, *Nat. Commun.*, 2015, **6**, 1–8.

71 Y. Li, M. Zhang, X. Guo, R. Wen, X. Li, X. Li, S. Li and L. Ma, Growth of high-quality covalent organic framework nanosheets at the interface of two miscible organic solvents, *Nanoscale Horiz.*, 2018, **3**, 205–212.

72 M. Pfeffermann, R. Dong, R. Graf, W. Zajaczkowski, T. Gorelik, W. Pisula, A. Narita, K. Müllen and X. Feng, Free-Standing Monolayer Two-Dimensional Supramolecular Organic Framework with Good Internal Order, *J. Am. Chem. Soc.*, 2015, **137**, 14525–14532.

73 Z. Wang, Q. Yu, Y. Huang, H. An, Y. Zhao, Y. Feng, X. Li, X. Shi, J. Liang, F. Pan, P. Cheng, Y. Chen, S. Ma and Z. Zhang, PolyCOFs: A New Class of Freestanding Responsive Covalent Organic Framework Membranes with High Mechanical Performance, *ACS Cent. Sci.*, 2019, DOI: 10.1021/acscentsci.9b00212.

74 F. Wang, L. Valentino, A. R. Corcos, G. M. Stiehl, B. J. Mariñas, D. C. Ralph, W. R. Dichtel, H. B. Balch and M. Matsumoto, Lewis-Acid-Catalyzed Interfacial Polymerization of Covalent Organic Framework Films, *Chem*, 2018, **4**, 308–317.

75 T. Rodenas, I. Luz, G. Prieto, B. Seoane, H. Miro, A. Corma, F. Kapteijn, F. X. Llabrés I Xamena and J. Gascon, Metal-organic framework nanosheets in polymer composite materials for gas separation, *Nat. Mater.*, 2015, **14**, 48–55.

76 I.-F. Chen, C.-F. Lu and W.-F. Su, Highly Conductive 2D Metal–Organic Framework Thin Film Fabricated by Liquid–Liquid Interfacial Reaction Using One-Pot-Synthesized Benzenehexathiol, *Langmuir*, 2018, **34**, 15754–15762.

77 M. Zhao, Y. Wang, Q. Ma, Y. Huang, X. Zhang, J. Ping, Z. Zhang, Q. Lu, Y. Yu, H. Xu, Y. Zhao and H. Zhang, Ultrathin 2D Metal-Organic Framework Nanosheets, *Adv. Mater.*, 2015, **27**, 7372–7378.

78 F. Xue, P. Kumar, W. Xu, K. A. Mkhoyan and M. Tsapatsis, Direct Synthesis of 7 nm-Thick Zinc(II)-Benzimidazole-Acetate Metal-Organic Framework Nanosheets, *Chem. Mater.*, 2018, **30**, 69–73.

79 G. Xu, T. Yamada, K. Otsubo, S. Sakaida and H. Kitagawa, Facile 'modular assembly' for fast construction of a highly oriented crystalline MOF nanofilm, *J. Am. Chem. Soc.*, 2012, **134**, 16524–16527.

80 V. Rubio-Giménez, S. Tatay, F. Volatron, F. J. Martínez-Casado, C. Martí-Gastaldo and E. Coronado, High-Quality Metal-Organic Framework Ultrathin Films for Electronically Active Interfaces, *J. Am. Chem. Soc.*, 2016, **138**, 2576–2584.

81 J. L. Zhuang, A. Terfort and C. Wöll, Formation of oriented and patterned films of metal-organic frameworks by liquid phase epitaxy: a review, *Coord. Chem. Rev.*, 2016, **307**, 391–424.

82 T. Haraguchi, K. Otsubo and H. Kitagawa, Emergence of Surface- and Interface-Induced Structures and Properties in Metal–Organic Framework Thin Films, *Eur. J. Inorg. Chem.*, 2018, **2018**, 1697–1706.

83 W. Guo, M. Zha, Z. Wang, E. Redel, Z. Xu and C. Wöll, Improving the Loading Capacity of Metal-Organic Framework Thin Films Using Optimized Linkers, *ACS Appl. Mater. Interfaces*, 2016, **8**, 24699–24702.

84 J. Liu, T. Wächter, A. Irmler, P. G. Weidler, H. Gliemann, F. Pauly, V. Mugnaini, M. Zharnikov and C. Wöll, Electric transport properties of surface-anchored metal-organic frameworks and the effect of ferrocene loading, *ACS Appl. Mater. Interfaces*, 2015, **7**, 9824–9830.

85 J. Liu, M. Paradinas, L. Heinke, M. Buck, C. Ocal, V. Mugnaini and C. Wöll, Film Quality and Electronic Properties of a Surface-Anchored Metal-Organic Framework Revealed by using a Multi-technique Approach, *ChemElectroChem*, 2016, **3**, 713–718.

86 D. Van Gough, T. N. Lambert, D. R. Wheeler, M. A. Rodriguez, M. T. Brumbach, M. D. Allendorf and E. D. Spoerke, Controlled nucleation and growth of pillared paddlewheel framework nanostacks onto chemically modified surfaces, *ACS Appl. Mater. Interfaces*, 2014, **6**, 1509–1514.

87 V. Stavila, J. Volponi, A. M. Katzenmeyer, M. C. Dixon and M. D. Allendorf, Kinetics and mechanism of metal–organic framework thin film growth: systematic investigation of HKUST-1 deposition on QCM electrodes, *Chem. Sci.*, 2012, **3**, 1531.

88 M. Framework, A. A. Talin, A. Centrone, A. C. Ford, M. E. Foster, V. Stavila, P. Haney, R. A. Kinney, V. Szalai, F. E. Gabaly, H. P. Yoon, F. Léonard and M. D. Allendorf, Tunable Electrical Conductivity in Metal-Organic Framework Thin-Film Devices, *Science*, 2014, **343**, 66–70.

89 S. Wannapaiboon, K. Sumida, K. Dilchert, M. Tu, S. Kitagawa, S. Furukawa and R. A. Fischer, Enhanced properties of metal-organic framework thin films fabricated: via a coordination modulation-controlled layer-by-layer process, *J. Mater. Chem. A*, 2017, **5**, 13665–13673.

90 J. F. Stoddart, X. Gong, G. Wang, C. Cheng, C.-W. Kung, A. Facchetti, J.-M. Han, A. C.-H. Sue, T. J. Marks, Z. Liu, K. Cai, O. K. Farha, Y. Y. Botros, Y. Shi, P. Li, H. Chen, Q.-H. Guo and D. Shen, Epitaxial Growth of γ-Cyclodextrin-Containing Metal–Organic Frameworks Based on a Host–Guest Strategy, *J. Am. Chem. Soc.*, 2018, **140**, 11402–11407.

91 G. Lu, O. K. Farha, W. Zhang, F. Huo and J. T. Hupp, Engineering ZIF-8 thin films for hybrid MOF-based devices, *Adv. Mater.*, 2012, **24**, 3970–3974.

92 H. Ji, S. Hwang, K. Kim, C. Kim and N. C. Jeong, Direct in Situ Conversion of Metals into Metal-Organic Frameworks: A Strategy for the Rapid Growth of MOF Films on Metal Substrates, *ACS Appl. Mater. Interfaces*, 2016, **8**, 32414–32420.

93 D. Kim and A. Coskun, Graphene oxide-templated preferential growth of continuous MOF thin films, *CrystEngComm*, 2016, **18**, 4013–4017.

94 K. Sakata, S. Kashiyama, G. Matsuo, S. Uemura, N. Kimizuka and M. Kunitake, Growth of Two-Dimensional Metal–Organic Framework Nanosheet Crystals on Graphite Substrates by Thermal Equilibrium

Treatment in Acetic Acid Vapor, *ChemNanoMat*, 2015, **1**, 259–263.

95 B. Hoppe, K. D. J. Hindricks, D. P. Warwas, H. A. Schulze, A. Mohmeyer, T. J. Pinkvos, S. Zailskas, M. R. Krey, C. Belke, S. König, M. Fröba, R. J. Haug and P. Behrens, Graphene-like metal-organic frameworks: morphology control, optimization of thin film electrical conductivity and fast sensing applications, *CrystEngComm*, 2018, **20**, 6458–6471.

96 V. Chernikova, O. Shekhah and M. Eddaoudi, Advanced Fabrication Method for the Preparation of MOF Thin Films: Liquid-Phase Epitaxy Approach Meets Spin Coating Method, *ACS Appl. Mater. Interfaces*, 2016, **8**, 20459–20464.

97 M. C. So, S. Jin, H.-J. Son, G. P. Wiederrecht, O. K. Farha and J. T. Hupp, Layer-by-layer fabrication of oriented porous thin films based on porphyrin-containing metal-organic frameworks, *J. Am. Chem. Soc.*, 2013, **135**, 15698–15701.

98 Y. Wang, L. Li, L. Yan, X. Gu, P. Dai, D. Liu, J. G. Bell, G. Zhao, X. Zhao and K. M. Thomas, Bottom-Up Fabrication of Ultrathin 2D Zr Metal-Organic Framework Nanosheets through a Facile Continuous Microdroplet Flow Reaction, *Chem. Mater.*, 2018, **30**, 3048–3059.

99 A. M. Evans, L. R. Parent, N. C. Flanders, R. P. Bisbey, E. Vitaku, L. X. Chen, N. C. Gianneschi and W. R. Dichtel, Seeded Growth of Single-Crystal Two-Dimensional Covalent Organic Frameworks, *Science*, 2018, 7883.

100 R. P. Bisbey, C. R. DeBlase, B. J. Smith and W. R. Dichtel, Two-dimensional Covalent Organic Framework Thin Films Grown in Flow, *J. Am. Chem. Soc.*, 2016, **138**, 11433–11436.

101 Y. Zhao, L. Guo, F. Gándara, Y. Ma, Z. Liu, C. Zhu, H. Lyu, C. A. Trickett, E. A. Kapustin, O. Terasaki and O. M. Yaghi, A Synthetic Route for Crystals of Woven Structures, Uniform Nanocrystals, and Thin Films of Imine Covalent Organic Frameworks, *J. Am. Chem. Soc.*, 2017, **139**, 13166–13172.

102 P. Serp, P. Kalck and R. Feurer, Chemical vapor deposition methods for the controlled preparation of supported catalytic materials, *Chem. Rev.*, 2002, **102**, 3085–3128.

103 Z. Cai, B. Liu, X. Zou and H. Cheng, Chemical Vapor Deposition Growth and Applications of Two-Dimensional Materials and Their Heterostructures, *Chem. Rev.*, 2018, **118**, 6091–6133.

104 P. C. Lemaire, J. Zhao, P. S. Williams, H. J. Walls, S. D. Shepherd, M. D. Losego, G. W. Peterson and G. N. Parsons, Copper Benzenetricarboxylate Metal-Organic Framework Nucleation Mechanisms on Metal Oxide Powders and Thin Films formed by Atomic Layer Deposition, *ACS Appl. Mater. Interfaces*, 2016, **8**, 9514–9522.

105 E. Ahvenniemi and M. Karppinen, Atomic/molecular layer deposition: a direct gas-phase route to crystalline metal-organic framework thin films, *Chem. Commun.*, 2016, **52**, 1139–1142.

106 E. Ahvenniemi and M. Karppinen, In Situ Atomic/Molecular Layer-by-Layer Deposition of Inorganic-Organic Coordination Network Thin Films from Gaseous Precursors, *Chem. Mater.*, 2016, **28**, 6260–6265.

107 E. Ahvenniemi and M. Karppinen, ALD/MLD processes for Mn and Co based hybrid thin films, *Dalton Trans.*, 2016, **45**, 10730.

108 L. D. Salmi, M. J. Heikkilä, E. Puukilainen, T. Sajavaara, D. Grosso and M. Ritala, Studies on atomic layer deposition of MOF-5 thin films, *Microporous Mesoporous Mater.*, 2013, **182**, 147–154.

109 I. Stassen, N. Campagnol, J. Fransaer, P. Vereecken, D. De Vos and R. Ameloot, Solvent-free synthesis of supported ZIF-8 films and patterns through transformation of deposited zinc oxide precursors, *CrystEngComm*, 2013, **15**, 9308–9311.

110 I. Stassen, M. Styles, G. Grenci, H. Van Gorp, W. Vanderlinden, S. De Feyter, P. Falcaro, D. De Vos, P. Vereecken and R. Ameloot, Chemical vapour deposition of zeolitic imidazolate framework thin films, *Nat. Mater.*, 2016, **15**, 304–310.

111 S. Spitzer, A. Rastgoo-Lahrood, K. MacKnapp, V. Ritter, S. Sotier, W. M. Heckl and M. Lackinger, Solvent-free on-surface synthesis of boroxine COF monolayers, *Chem. Commun.*, 2017, **53**, 5147–5150.

112 F. J. Claire, M. A. Solomos, J. Kim and T. Kempa, unpublished work.

113 M. M. Li, F. J. Claire, M. A. Solomos, S. M. Tenney, S. A. Ivanov, M. A. Siegler and T. J. Kempa, Molecular chains of coordinated dimolybdenum isonicotinate paddlewheel clusters, *RSC Adv.*, 2019, **9**, 16492–16495.

114 B. Garai, A. Mallick, A. Das, R. Mukherjee and R. Banerjee, Self-Exfoliated Metal-Organic Nanosheets through Hydrolytic Unfolding of Metal-Organic Polyhedra, *Chem.–Eur. J.*, 2017, **23**, 7361–7366.

115 S. Zhao, Y. Wang, J. Dong, C. T. He, H. Yin, P. An, K. Zhao, X. Zhang, C. Gao, L. Zhang, J. Lv, J. Wang, J. Zhang, A. M. Khattak, N. A. Khan, Z. Wei, J. Zhang, S. Liu, H. Zhao and Z. Tang, Ultrathin metal-organic framework nanosheets for electrocatalytic oxygen evolution, *Nat. Energy*, 2016, **1**, 1–10.

116 D. N. Bunck and W. R. Dichtel, Bulk synthesis of exfoliated two-dimensional polymers using hydrazone-linked covalent organic frameworks, *J. Am. Chem. Soc.*, 2013, **135**, 14952–14955.

117 Y. Zhao, L. Jiang, L. Shangguan, L. Mi, A. Liu and S. Liu, Synthesis of porphyrin-based two-dimensional metal-organic framework nanodisk with small size and few layers, *J. Mater. Chem. A*, 2018, **6**, 2828–2833.

118 J. Nicks, J. Zhang and J. A. Foster, Tandem catalysis by ultrathin metal–organic nanosheets formed through post-synthetic functionalisation of a layered framework, *Chem. Commun.*, 2019, **55**, 8788–8791.

119 V. K.-M. Au, K. Nakayashiki, H. Huang, S. Suginome, H. Sato and T. Aida, Stepwise Expansion of Layered Metal–Organic Frameworks for Nonstochastic Exfoliation into Porous Nanosheets, *J. Am. Chem. Soc.*, 2018, **141**, 53–57.

120 Z. Wang, J. Liu, B. Lukose, Z. Gu, P. G. Weidler, H. Gliemann, T. Heine and C. Wöll, Nanoporous designer solids with huge lattice constant gradients:

multiheteroepitaxy of metal-organic frameworks, *Nano Lett.*, 2014, **14**, 1526–1529.

121 I. Stassen, M. Styles, T. Van Assche, N. Campagnol, J. Fransaer, J. Denayer, J. C. Tan, P. Falcaro, D. De Vos and R. Ameloot, Electrochemical film deposition of the zirconium metal-organic framework uio-66 and application in a miniaturized sorbent trap, *Chem. Mater.*, 2015, **27**, 1801–1807.

122 J. W. Colson, A. R. Woll, A. Mukherjee, M. P. Levendorf, E. L. Spitler, V. B. Shields, M. G. Spencer, J. Park and W. R. Dichtel, Oriented 2D Covalent Organic Framework Thin Films on Single-Layer Graphene, *Science*, 2011, **332**, 228–232.

123 S. Motoyama, R. Makiura, O. Sakata and H. Kitagawa, Highly Crystalline Nanofilm by Layering of Porphyrin Metal-Organic Framework Sheets, *J. Am. Chem. Soc.*, 2011, **2**, 5640–5643.

124 R. Matsuoka, R. Toyoda, R. Shiotsuki, N. Fukui, K. Wada, H. Maeda, R. Sakamoto, S. Sasaki, H. Masunaga, K. Nagashio and H. Nishihara, Expansion of the Graphdiyne Family: A Triphenylene-Cored Analogue, *ACS Appl. Mater. Interfaces*, 2019, **11**, 2730–2733.

125 W. Lu and X. Wu, Ni-MOF nanosheet arrays: efficient non-noble-metal electrocatalysts for non-enzymatic monosaccharide sensing, *New J. Chem.*, 2018, **42**, 3180–3183.

126 A. Ayala, J. D. Tarver, K. E. Hurst, C. M. Brown, P. A. Parilla, T. Gennett, H. Z. H. Jiang, M. T. Kapelewski, J. R. Long, T. Runčevski and S. A. FitzGerald, Record High Hydrogen Storage Capacity in the Metal–Organic Framework Ni_2(m-dobdc) at Near-Ambient Temperatures, *Chem. Mater.*, 2018, **30**, 8179–8189.

127 S. Chandra, S. Kandambeth, B. P. Biswal, B. Lukose, S. M. Kunjir, M. Chaudhary, R. Babarao, T. Heine and R. Banerjee, Chemically stable multilayered covalent organic nanosheets from covalent organic frameworks via mechanical delamination, *J. Am. Chem. Soc.*, 2013, **135**, 17853–17861.

128 I. Berlanga, M. L. Ruiz-González, J. M. González-Calbet, J. L. G. Fierro, R. Mas-Ballesté and F. Zamora, Delamination of layered covalent organic frameworks, *Small*, 2011, **7**, 1207–1211.

129 D. D. Medina, V. Werner, F. Auras, R. Tautz, M. Dogru, J. Schuster, S. Linke, M. Döblinger, J. Feldmann, P. Knochel and T. Bein, Oriented thin films of a benzodithiophene covalent organic framework, *ACS Nano*, 2014, **8**, 4042–4052.

130 G. Li, K. Zhang and T. Tsuru, Two-Dimensional Covalent Organic Framework (COF) Membranes Fabricated via the Assembly of Exfoliated COF Nanosheets, *ACS Appl. Mater. Interfaces*, 2017, **9**, 8433–8436.

131 S. Wu, L. Qin, K. Zhang, Z. Xin and S. Zhao, Ultrathin 2D metal-organic framework nanosheets prepared via sonication exfoliation of membranes from interfacial growth and exhibition of enhanced catalytic activity by their gold nanocomposites, *RSC Adv.*, 2019, **9**, 9386–9391.

132 N. Lahiri, N. Lotfizadeh, R. Tsuchikawa, V. V. Deshpande and J. Louie, Hexaaminobenzene as a building block for a family of 2D coordination polymers, *J. Am. Chem. Soc.*, 2017, **139**, 19–22.

133 S. Kumar, J. A. Lee, S. Maheshwari, A. Mittal, C. Sung, M. Cococcioni, L. F. Francis, A. V. Mccormick, K. A. Mkhoyan and M. Tsapatsis, Dispersible Exfoliated Zeolite Nanosheets and Their Application as a Selective Membrane, *Science*, 2011, **734**, 72–76.

134 G. Zhan and H. C. Zeng, Synthesis and Functionalization of Oriented Metal–Organic-Framework Nanosheets : Toward a Series of 2D Catalysts, *Adv. Funct. Mater.*, 2016, **26**, 3268–3281.

135 T. He, B. Ni, S. Zhang, Y. Gong, H. Wang, L. Gu and J. Zhuang, Ultrathin 2D Zirconium Metal–Organic Framework Nanosheets : Preparation and Application in Photocatalysis, *Small*, 2018, **14**, 1–6.

136 A. Dmitriev, H. Spillmann, N. Lin, J. V. Barth and K. Kern, Modular assembly of two-dimensional metal-organic coordination networks at a metal surface, *Angew. Chem., Int. Ed.*, 2003, **42**, 2670–2673.

137 P. Amo-Ochoa, L. Welte, R. González-Prieto, P. J. Sanz Miguel, C. J. Gómez-García, E. Mateo-Martí, S. Delgado, J. Gómez-Herrero and F. Zamora, Single layers of a multifunctional laminar Cu(i,ii) coordination polymer, *Chem. Commun.*, 2010, **46**, 3262–3264.

138 L. Xu, X. Zhou, W. Q. Tian, T. Gao, Y. F. Zhang, S. Lei and Z. F. Liu, Surface-confined single-layer covalent organic framework on single-layer graphene grown on copper foil, *Angew. Chem., Int. Ed.*, 2014, **53**, 9564–9568.

139 C. Chen, T. Joshi, H. Li, A. D. Chavez, Z. Pedramrazi, P. N. Liu, H. Li, W. R. Dichtel, J. L. Bredas and M. F. Crommie, Local Electronic Structure of a Single-Layer Porphyrin-Containing Covalent Organic Framework, *ACS Nano*, 2018, **12**, 385–391.

140 C. W. Kung, K. Otake, C. T. Buru, S. Goswami, Y. Cui, J. T. Hupp, A. M. Spokoyny and O. K. Farha, Increased Electrical Conductivity in a Mesoporous Metal-Organic Framework Featuring Metallacarboranes Guests, *J. Am. Chem. Soc.*, 2018, **140**, 3871–3875.

141 M. S. Yao, X. J. Lv, Z. H. Fu, W. H. Li, W. H. Deng, G. D. Wu and G. Xu, Layer-by-Layer Assembled Conductive Metal–Organic Framework Nanofilms for Room-Temperature Chemiresistive Sensing, *Angew. Chem., Int. Ed.*, 2017, **56**, 16510–16514.

142 T. Kambe, R. Sakamoto, T. Kusamoto, T. Pal, N. Fukui, K. Hoshiko, T. Shimojima, Z. Wang, T. Hirahara, K. Ishizaka, S. Hasegawa, F. Liu and H. Nishihara, Redox control and high conductivity of nickel bis(dithiolene) complex π-nanosheet: a potential organic two-dimensional topological insulator, *J. Am. Chem. Soc.*, 2014, **136**, 14357–14360.

143 Y. Wu, S. J. Moorhouse and D. O'Hare, Time-Resolved in Situ Diffraction Reveals a Solid-State Rearrangement during Solvothermal MOF Synthesis, *Chem. Mater.*, 2015, **27**, 7236–7239.

144 J. Cravillon, C. A. Schröder, R. Nayuk, J. Gummel, K. Huber and M. Wiebcke, Fast nucleation and growth of ZIF-8 nanocrystals monitored by time-resolved in situ small-angle and wide-angle X-ray scattering, *Angew. Chem., Int. Ed.*, 2011, **50**, 8067–8071.

145 M. W. Terban, D. Banerjee, S. Ghose, B. Medasani, A. Shukla, B. A. Legg, Y. Zhou, Z. Zhu, M. L. Sushko, J. J. De Yoreo, J. Liu, P. K. Thallapally and S. J. L. Billinge, Early stage structural development of prototypical zeolitic imidazolate framework (ZIF) in solution, *Nanoscale*, 2018, **10**, 4291–4300.

146 M. M. Biener, J. Biener, R. Schalek and C. M. Friend, Growth of nanocrystalline on Au (111) studied by in situ scanning tunneling microscopy tunneling microscopy, *J. Chem. Phys.*, 2004, **121**, 12010–12016.

147 S. H. Dave, C. Gong, A. W. Robertson, J. H. Warner and C. Grossman, Chemistry and Structure of Graphene Oxide via Direct Imaging, *ACS Nano*, 2016, **10**, 7515–7522.

148 L. D. B. Mandemaker, M. Filez, G. Delen, H. Tan, X. Zhang, D. Lohse and B. M. Weckhuysen, Time-Resolved in Situ Liquid-Phase Atomic Force Microscopy and Infrared Nanospectroscopy during the Formation of Metal-Organic Framework Thin Films, *J. Phys. Chem. Lett.*, 2018, **9**, 1838–1844.

149 J. Zhao, B. Kalanyan, H. F. Barton, B. A. Sperling, G. N. Parsons, N. Carolina and U. States, In Situ Time-Resolved Attenuated Total Reflectance Infrared Spectroscopy for Probing Metal−Organic Framework Thin Film Growth, *Chem. Mater.*, 2017, **29**, 8804–8810.

150 A. J. Clough, J. W. Yoo, M. H. Mecklenburg and S. C. Marinescu, Two-dimensional metal-organic surfaces for efficient hydrogen evolution from water, *J. Am. Chem. Soc.*, 2015, **137**, 118–121.

151 R. Dong, M. Pfeffermann, H. Liang, Z. Zheng, X. Zhu, J. Zhang and X. Feng, Large-Area, Free-Standing, Two-Dimensional Supramolecular Polymer Single-Layer Sheets for Highly Efficient Electrocatalytic Hydrogen Evolution, *Angew. Chem., Int. Ed.*, 2015, **54**, 12058–12063.

152 C. A. Downes, A. J. Clough, K. Chen, J. W. Yoo and S. C. Marinescu, Evaluation of the H_2 Evolving Activity of Benzenehexathiolate Coordination Frameworks and the Effect of Film Thickness on H_2 Production, *ACS Appl. Mater. Interfaces*, 2018, **10**, 1719–1727.

153 X. Sun, K. H. Wu, R. Sakamoto, T. Kusamoto, H. Maeda, X. Ni, W. Jiang, F. Liu, S. Sasaki, H. Masunaga and H. Nishihara, Bis(aminothiolato)nickel nanosheet as a redox switch for conductivity and an electrocatalyst for the hydrogen evolution reaction, *Chem. Sci.*, 2017, **8**, 8078–8085.

154 D. Zhu, J. Liu, Y. Zhao, Y. Zheng and S. Z. Qiao, Engineering 2D Metal–Organic Framework/MoS_2 Interface for Enhanced Alkaline Hydrogen Evolution, *Small*, 2019, **15**, 1–8.

155 J. Duan, S. Chen and C. Zhao, Ultrathin metal-organic framework array for efficient electrocatalytic water splitting, *Nat. Commun.*, 2017, **8**, 1–7.

156 F.-L. Li, P. Wang, X. Huang, D. J. Young, H.-F. Wang, P. Braunstein and J.-P. Lang, Large-Scale, Bottom-Up Synthesis of Binary Metal-Organic Framework Nanosheets for Efficient Water Oxidation, *Angew. Chem., Int. Ed.*, 2019, **58**, 7051–7056.

157 E. M. Miner, T. Fukushima, D. Sheberla, L. Sun, Y. Surendranath and M. Dincă, Electrochemical oxygen reduction catalysed by Ni_3(hexaiminotriphenylene)$_2$, *Nat. Commun.*, 2016, **7**, 1–7.

158 N. Kornienko, Y. Zhao, C. S. Kley, C. Zhu, D. Kim, S. Lin, C. J. Chang, O. M. Yaghi and P. Yang, Metal-Organic Frameworks for Electrocatalytic Reduction of Carbon Dioxide, *J. Am. Chem. Soc.*, 2015, **137**, 14129–14135.

159 I. Hod, M. D. Sampson, P. Deria, C. P. Kubiak, O. K. Farha and J. T. Hupp, Fe-Porphyrin-Based Metal-Organic Framework Films as High-Surface Concentration, Heterogeneous Catalysts for Electrochemical Reduction of CO_2, *ACS Catal.*, 2015, **5**, 6302–6309.

160 Y. Huang, M. Zhao, S. Han, Z. Lai, J. Yang, C. Tan, Q. Ma, Q. Lu, J. Chen, X. Zhang, Z. Zhang, B. Li, B. Chen, Y. Zong and H. Zhang, Growth of Au Nanoparticles on 2D Metalloporphyrinic Metal-Organic Framework Nanosheets Used as Biomimetic Catalysts for Cascade Reactions, *Adv. Mater.*, 2017, **29**, 1–5.

161 K. Rui, G. Zhao, Y. Chen, Y. Lin, Q. Zhou, J. Chen, J. Zhu, W. Sun, W. Huang and S. X. Dou, Hybrid 2D Dual-Metal–Organic Frameworks for Enhanced Water Oxidation Catalysis, *Adv. Funct. Mater.*, 2018, **28**, 1–9.

162 W. Xia, A. Mahmood, R. Zou and Q. Xu, Metal-organic frameworks and their derived nanostructures for electrochemical energy storage and conversion, *Energy Environ. Sci.*, 2015, **8**, 1837–1866.

163 J. G. Park, M. L. Aubrey, J. Oktawiec, K. Chakarawet, L. E. Darago, F. Grandjean, G. J. Long and J. R. Long, Charge Delocalization and Bulk Electronic Conductivity in the Mixed-Valence Metal-Organic Framework Fe(1,2,3-triazolate)$_2$(BF_4)$_x$, *J. Am. Chem. Soc.*, 2018, **140**, 8526–8534.

164 P. Silva, S. M. F. Vilela, J. P. C. Tomé and F. A. Almeida Paz, Multifunctional metal–organic frameworks: from academia to industrial applications, *Chem. Soc. Rev.*, 2015, **44**, 6774–6803.

165 D. Feng, T. Lei, M. R. Lukatskaya, J. Park, Z. Huang, M. Lee, L. Shaw, S. Chen, A. A. Yakovenko, A. Kulkarni, J. Xiao, K. Fredrickson, J. B. Tok, X. Zou, Y. Cui and Z. Bao, Robust and conductive two-dimensional metal-organic frameworks with exceptionally high volumetric and areal capacitance, *Nat. Energy*, 2018, **3**, 30–36.

166 L. S. Xie, L. Sun, R. Wan, S. S. Park, J. A. DeGayner, C. H. Hendon, M. Dincă, M. Dincă, J. A. DeGayner, C. H. Hendon, R. Wan, S. S. Park and L. S. Xie, Tunable Mixed-Valence Doping toward Record Electrical Conductivity in a Three-Dimensional Metal-Organic Framework, *J. Am. Chem. Soc.*, 2018, **140**, 7411–7414.

167 A. J. Clough, J. M. Skelton, C. A. Downes, A. A. De La Rosa, J. W. Yoo, A. Walsh, B. C. Melot and S. C. Marinescu, Metallic Conductivity in a Two-Dimensional Cobalt Dithiolene Metal-Organic Framework, *J. Am. Chem. Soc.*, 2017, **139**, 10863–10867.

168 M. A. Blood-Forsythe, C. R. Wade, A. Aspuru-Guzik, M. Dincă, C. K. Brozek, D. Sheberla, L. Sun and S. Er, High Electrical Conductivity in Ni_3(2,3,6,7,10,11-hexaiminotriphenylene)$_2$, a Semiconducting Metal–Organic Graphene Analogue, *J. Am. Chem. Soc.*, 2014, **136**, 8859–8862.

169 S. Chandra, D. Roy Chowdhury, M. Addicoat, T. Heine, A. Paul and R. Banerjee, Molecular Level Control of the Capacitance of Two-Dimensional Covalent Organic Frameworks: Role of Hydrogen Bonding in Energy Storage Materials, *Chem. Mater.*, 2017, **29**, 2074–2080.

170 R. Dong, P. Han, H. Arora, M. Ballabio, M. Karakus, Z. Zhang, C. Shekhar, P. Adler, P. S. Petkov, A. Erbe, S. C. B. Mannsfeld, C. Felser, T. Heine, M. Bonn, X. Feng and E. Cánovas, High-mobility band-like charge transport in a semiconducting two-dimensional metal–organic framework, *Nat. Mater.*, 2018, **17**, 1027–1032.

171 G. Wu, J. Huang, Y. Zang, J. He and G. Xu, Porous field-effect transistors based on a semiconductive metal-organic framework, *J. Am. Chem. Soc.*, 2017, **139**, 1360–1363.

172 C. R. Deblase, K. Hernández-Burgos, K. E. Silberstein, G. G. Rodríguez-Calero, R. P. Bisbey, H. D. Abruña and W. R. Dichtel, Rapid and efficient redox processes within 2D covalent organic framework thin films, *ACS Nano*, 2015, **9**, 3178–3183.

173 D. Sheberla, J. C. Bachman, J. S. Elias, C. J. Sun, Y. Shao-Horn and M. Dincă, Conductive MOF electrodes for stable supercapacitors with high areal capacitance, *Nat. Mater.*, 2017, **16**, 220–224.

174 H. Chen, H. Tu, C. Hu, Y. Liu, D. Dong, Y. Sun, Y. Dai, S. Wang, H. Qian, Z. Lin and L. Chen, Cationic Covalent Organic Framework Nanosheets for Fast Li-Ion Conduction, *J. Am. Chem. Soc.*, 2018, **140**, 896–899.

175 S. Wang, Q. Wang, P. Shao, Y. Han, X. Gao, L. Ma, S. Yuan, X. Ma, J. Zhou, X. Feng and B. Wang, Exfoliation of Covalent Organic Frameworks into Few-Layer Redox-Active Nanosheets as Cathode Materials for Lithium-Ion Batteries, *J. Am. Chem. Soc.*, 2017, **139**, 4258–4261.

176 C. R. Mulzer, L. Shen, R. P. Bisbey, J. R. McKone, N. Zhang, H. D. Abruña and W. R. Dichtel, Superior charge storage and power density of a conducting polymer-modified covalent organic framework, *ACS Cent. Sci.*, 2016, **2**, 667–673.

177 S. Rana, R. Rajendra, B. Dhara, P. K. Jha and N. Ballav, Highly Hydrophobic and Chemically Rectifiable Surface-Anchored Metal-Organic Framework Thin-Film Devices, 2016, **3**, 1–8.

178 L. J. Han, D. Zheng, S. G. Chen, H. G. Zheng and J. Ma, A Highly Solvent-Stable Metal–Organic Framework Nanosheet: Morphology Control, Exfoliation, and Luminescent Property, *Small*, 2018, **14**, 1–7.

179 H. Xu, J. Gao, X. Qian, J. Wang, H. He, Y. Cui, Y. Yang, Z. Wang and G. Qian, Metal-organic framework nanosheets for fast-response and highly sensitive luminescent sensing of Fe^{3+}, *J. Mater. Chem. A*, 2016, **4**, 10900–10905.

180 M. G. Campbell and M. Dincă, Metal–organic frameworks as active materials in electronic sensor devices, *Sensors*, 2017, **17**, 1–11.

181 M. K. Smith and K. A. Mirica, Self-Organized Frameworks on Textiles (SOFT): Conductive Fabrics for Simultaneous Sensing, Capture, and Filtration of Gases, *J. Am. Chem. Soc.*, 2017, **139**, 16759–16767.

182 M. K. Smith, K. E. Jensen, P. A. Pivak and K. A. Mirica, Direct Self-Assembly of Conductive Nanorods of Metal-Organic Frameworks into Chemiresistive Devices on Shrinkable Polymer Films, *Chem. Mater.*, 2016, **28**, 5264–5268.

183 Z. Meng, A. Aykanat and K. A. Mirica, Welding Metallophthalocyanines into Bimetallic Molecular Meshes for Ultrasensitive, Low-Power Chemiresistive Detection of Gases, *J. Am. Chem. Soc.*, 2018, **141**, 2046–2053.

184 A. M. Ullman, C. G. Jones, F. P. Doty, V. Stavila, A. A. Talin and M. D. Allendorf, Hybrid Polymer/Metal–Organic Framework Films for Colorimetric Water Sensing over a Wide Concentration Range, *ACS Appl. Mater. Interfaces*, 2018, **10**, 24201–24208.

185 M. R. Tchalala, Y. Belmabkhout, K. Adil, K. N. Chappanda, A. Cadiau, P. M. Bhatt, K. N. Salama and M. Eddaoudi, Concurrent Sensing of CO_2 and H_2O from Air Using Ultramicroporous Fluorinated Metal-Organic Frameworks: Effect of Transduction Mechanism on the Sensing Performance, *ACS Appl. Mater. Interfaces*, 2019, **11**, 1706–1712.

186 M. G. Campbell, D. Sheberla, S. F. Liu, T. M. Swager and M. Dincă, Cu_3(hexaiminotriphenylene)$_2$: an electrically conductive 2D metal-organic framework for chemiresistive sensing, *Angew. Chem., Int. Ed.*, 2015, **54**, 4349–4352.

187 Z. Li, L. Qiu, W. Wang, T. Xu, Y. Wu and X. Jiang, Fabrication of nanosheets of a fluorescent metal–organic framework $[Zn(BDC)(H_2O)]_n$ (BDC = 1,4-benzenedicarboxylate): ultrasonic synthesis and sensing of ethylamine, *Inorg. Chem. Commun.*, 2008, **11**, 1375–1377.

188 C. Zhang, S. Zhang, Y. Yan, F. Xia, A. Huang and Y. Xian, Highly Fluorescent Polyimide Covalent Organic Nanosheets as Sensing Probes for the Detection of 2,4,6-Trinitrophenol, 2017, **9**, 13415–13421.

189 Y. Peng, Y. Huang, Y. Zhu, B. Chen, L. Wang, Z. Lai, Z. Zhang, M. Zhao, C. Tan, N. Yang, F. Shao, Y. Han and H. Zhang, Ultrathin Two-Dimensional Covalent Organic Framework Nanosheets: Preparation and Application in Highly Sensitive and Selective DNA Detection, *J. Am. Chem. Soc.*, 2017, **139**, 8698–8704.

190 C. He, K. Lu and W. Lin, Nanoscale metal-organic frameworks for real-time intracellular pH sensing in live cells, *J. Am. Chem. Soc.*, 2014, **136**, 12253–12256.

191 R. Xu, Y. Wang, X. Duan, K. Lu, D. Micheroni, A. Hu and W. Lin, Nanoscale Metal-Organic Frameworks for Ratiometric Oxygen Sensing in Live Cells, *J. Am. Chem. Soc.*, 2016, **138**, 2158–2161.

192 Y. Wang, M. Zhao, J. Ping, B. Chen, X. Cao, Y. Huang, C. Tan, Q. Ma, S. Wu, Y. Yu, Q. Lu, J. Chen, W. Zhao,

Y. Ying and H. Zhang, Bioinspired Design of Ultrathin 2D Bimetallic Metal-Organic-Framework Nanosheets Used as Biomimetic Enzymes, *Adv. Mater.*, 2016, **28**, 4149–4155.

193 J. Zhu, J. Hou, A. Uliana, Y. Zhang, M. Tian and B. Van Der Bruggen, The rapid emergence of two-dimensional nanomaterials for high-performance separation membranes, *J. Mater. Chem. A*, 2018, **6**, 3773–3792.

194 Z. Y. Yeo, S. P. Chai, P. W. Zhu and A. R. Mohamed, An overview: synthesis of thin films/membranes of metal organic frameworks and its gas separation performances, *RSC Adv.*, 2014, **4**, 54322–54334.

195 D. J. Babu, G. He, L. F. Villalobos and K. V. Agrawal, Crystal Engineering of Metal-Organic Framework Thin Films for Gas Separations, *ACS Sustainable Chem. Eng.*, 2019, **7**, 49–69.

196 X. Li, Y. Liu, J. Wang, J. Gascon, J. Li and B. Van Der Bruggen, Metal-organic frameworks based membranes for liquid separation, *Chem. Soc. Rev.*, 2017, **46**, 7124–7144.

197 H. Yang, L. Yang, H. Wang, Z. Xu, Y. Zhao, Y. Luo, N. Nasir, Y. Song, H. Wu, F. Pan and Z. Jiang, Covalent organic framework membranes through a mixed-dimensional assembly for molecular separations, *Nat. Commun.*, 2019, **10**, 1–10.

198 M. Wang, F. Pan, H. Yang, Y. Cao, H. Wang, Y. Song, Z. Lu, M. Sun, H. Wu and Z. Jiang, Constructing channel-mediated facilitated transport membranes by incorporating covalent organic framework nanosheets with tunable microenvironments, *J. Mater. Chem. A*, 2019, **7**, 9912–9923.

199 P. Albacete, A. López-Moreno, S. Mena-Hernando, A. E. Platero-Prats, E. M. Pérez and F. Zamora, Chemical sensing of water contaminants by a colloid of a fluorescent imine-linked covalent organic framework, *Chem. Commun.*, 2019, **55**, 1382–1385.

200 Z. G. Gu, W. Q. Fu, X. Wu and J. Zhang, Liquid-phase epitaxial growth of a homochiral MOF thin film on poly(l-DOPA) functionalized substrate for improved enantiomer separation, *Chem. Commun.*, 2016, **52**, 772–775.

201 J. Guo, Y. Zhang, Y. Zhu, C. Long, M. Zhao, M. He, X. Zhang, J. Lv, B. Han and Z. Tang, Chiral MOFs Very Important Paper Ultrathin Chiral Metal–Organic-Framework Nanosheets for Efficient Enantioselective Separation, *Angew. Chem., Int. Ed.*, 2018, 6873–6877, DOI: 10.1002/anie.201803125.

202 X. Wu, X. Han, Q. Xu, Y. Liu, C. Yuan, S. Yang, Y. Liu, J. Jiang and Y. Cui, Chiral BINOL-Based Covalent Organic Frameworks for Enantioselective Sensing, *J. Am. Chem. Soc.*, 2019, **141**, 7081–7089.

203 H. Ang and L. Hong, Polycationic Polymer-Regulated Assembling of 2D MOF Nanosheets for High-Performance Nanofiltration, *ACS Appl. Mater. Interfaces*, 2017, **9**, 28079–28088.

204 S. Kandambeth, B. P. Biswal, H. D. Chaudhari, K. C. Rout, U. K. Kharul and R. Banerjee, Selective Molecular Sieving in Self-Standing Porous Covalent-Organic-Framework Membranes, 2017, **29**, 1–9.

205 K. Dey, M. Pal, K. C. Rout, S. S. Kunjattu, A. Das, R. Mukherjee, U. K. Kharul and R. Banerjee, Selective Molecular Separation by Interfacially Crystallized Covalent Organic Framework Thin Films, *J. Am. Chem. Soc.*, 2017, **139**, 13083–13091.

206 D. Cohen-Tanugi and J. C. Grossman, Water desalination across nanoporous graphene, *Nano Lett.*, 2012, **12**, 3602–3608.

207 L. C. Lin, J. Choi and J. C. Grossman, Two-dimensional covalent triazine framework as an ultrathin-film nanoporous membrane for desalination, *Chem. Commun.*, 2015, **51**, 14921–14924.

208 W. Zhou, M. Wei, X. Zhang, F. Xu and Y. Wang, Fast Desalination by Multilayered Covalent Organic Framework (COF) Nanosheets, *ACS Appl. Mater. Interfaces*, 2019, **11**, 16847–16854.

209 X. Liu, N. K. Demir, Z. Wu and K. Li, Highly Water-Stable Zirconium Metal-Organic Framework UiO-66 Membranes Supported on Alumina Hollow Fibers for Desalination, *J. Am. Chem. Soc.*, 2015, **137**, 6999–7002.

210 X. Wang, L. Zhai, Y. Wang, R. Li, X. Gu, Y. D. Yuan, Y. Qian, Z. Hu and D. Zhao, Improving Water-Treatment Performance of Zirconium Metal-Organic Framework Membranes by Postsynthetic Defect Healing, *ACS Appl. Mater. Interfaces*, 2017, **9**, 37848–37855.

211 X. Wang, C. Chi, K. Zhang, Y. Qian, K. M. Gupta, Z. Kang, J. Jiang and D. Zhao, Reversed thermo-switchable molecular sieving membranes composed of two-dimensional metal-organic nanosheets for gas separation, *Nat. Commun.*, 2017, **8**, 1–10.

212 P. Szilágyi, R. J. Westerwaal, M. Lansink, H. I. Van Montfort, B. J. Trześniewski, M. V. Garcia, H. Geerlings and B. Dam, Contaminant-resistant MOF-Pd composite for H_2 separation, *RSC Adv.*, 2015, **5**, 89323–89326.

213 Z. P. Smith, J. E. Bachman, T. Li, B. Gludovatz, V. A. Kusuma, T. Xu, D. P. Hopkinson, R. O. Ritchie and J. R. Long, Increasing M_2(dobdc) Loading in Selective Mixed-Matrix Membranes: A Rubber Toughening Approach, *Chem. Mater.*, 2018, **30**, 1484–1495.

214 Z. Kang, Y. Peng, Y. Qian, D. Yuan, M. A. Addicoat, T. Heine, Z. Hu, L. Tee, Z. Guo and D. Zhao, Mixed Matrix Membranes (MMMs) Comprising Exfoliated 2D Covalent Organic Frameworks (COFs) for Efficient CO_2 Separation, *Chem. Mater.*, 2016, **28**, 1277–1285.

215 K. Duan, J. Wang, Y. Zhang and J. Liu, Covalent organic frameworks (COFs) functionalized mixed matrix membrane for effective CO_2/N_2 separation, *J. Membr. Sci.*, 2019, **572**, 588–595.

216 P. Chandrasekhar, A. Mukhopadhyay, G. Savitha and J. N. Moorthy, Orthogonal self-assembly of a trigonal triptycene triacid: signaling of exfoliation of porous 2D metal-organic layers by fluorescence and selective CO_2 capture by the hydrogen-bonded MOF, *J. Mater. Chem. A*, 2017, **5**, 5402–5412.

217 M. H. Pham, G. T. Vuong, F. G. Fontaine and T. O. Do, Rational synthesis of metal-organic framework nanocubes and nanosheets using selective modulators and their

morphology-dependent gas-sorption properties, *Cryst. Growth Des.*, 2012, **12**, 3091–3095.

218 Y. Lo, C. H. Lam, C. W. Chang, A. C. Yang and D. Y. Kang, Polymorphism/pseudopolymorphism of metal-organic frameworks composed of zinc(II) and 2-methylimidazole: synthesis, stability, and application in gas storage, *RSC Adv.*, 2016, **6**, 89148–89156.

219 D. Kim, D. W. Kim, W. G. Hong and A. Coskun, Graphene/ZIF-8 composites with tunable hierarchical porosity and electrical conductivity, *J. Mater. Chem. A*, 2016, **4**, 7710–7717.

220 R. Kumar, K. Jayaramulu, T. K. Maji and C. N. R. Rao, Growth of 2D sheets of a MOF on graphene surfaces to yield composites with novel gas adsorption characteristics, *Dalton Trans.*, 2014, **43**, 7383–7386.

221 H. Li, J. Hou, T. D. Bennett, J. Liu and Y. Zhang, Templated growth of vertically aligned 2D metal-organic framework nanosheets, *J. Mater. Chem. A*, 2019, **7**, 5811–5818.

222 P. Á. Szilágyi, R. J. Westerwaal, R. Van De Krol, H. Geerlings and B. Dam, Metal-organic framework thin films for protective coating of Pd-based optical hydrogen sensors, *J. Mater. Chem. C*, 2013, **1**, 8146–8155.

223 K. Liang, J. J. Richardson, C. J. Doonan, X. Mulet, Y. Ju, J. Cui, F. Caruso and P. Falcaro, An Enzyme-Coated Metal–Organic Framework Shell for Synthetically Adaptive Cell Survival, *Angew. Chem., Int. Ed.*, 2017, **56**, 8510–8515.

224 M. Hanke, H. K. Arslan, S. Bauer, O. Zybaylo, C. Christophis, H. Gliemann, A. Rosenhahn and C. Wöll, The biocompatibility of metal-organic framework coatings: an investigation on the stability of SURMOFs with regard to water and selected cell culture media, *Langmuir*, 2012, **28**, 6877–6884.

225 M. Tsotsalas, J. Liu, B. Tettmann, S. Grosjean, A. Shahnas, Z. Wang, C. Azucena, M. Addicoat, T. Heine, J. Lahann, J. Overhage, S. Bra, H. Gliemann and C. Wo, Fabrication of Highly Uniform Gel Coatings by the Conversion of Surface-Anchored Metal–Organic Frameworks, 2014, **136**, 8–11.

226 C. T. Buru, M. B. Majewski, A. J. Howarth, R. H. Lavroff, C. W. Kung, A. W. Peters, S. Goswami and O. K. Farha, Improving the Efficiency of Mustard Gas Simulant Detoxification by Tuning the Singlet Oxygen Quantum Yield in Metal-Organic Frameworks and Their Corresponding Thin Films, *ACS Appl. Mater. Interfaces*, 2018, **10**, 23802–23806.

227 P. De Luna, W. Liang, A. Mallick, O. Shekhah, F. P. García De Arquer, A. H. Proppe, P. Todorović, S. O. Kelley, E. H. Sargent and M. Eddaoudi, Metal-Organic Framework Thin Films on High-Curvature Nanostructures Toward Tandem Electrocatalysis, *ACS Appl. Mater. Interfaces*, 2018, **10**, 31225–31232.

